Title

Zinc/Air Battery R & D Research and Development of Bifunctional Oxygen Electrode Tasks I and II. Final Report

Authors

Klein, M

Viswanathan, S

Publication Date

1986-12-01

LBL-22661 c.2
UC-94c

Lawrence Berkeley Laboratory
UNIVERSITY OF CALIFORNIA

APPLIED SCIENCE DIVISION

ZINC/AIR BATTERY R & D
RESEARCH AND DEVELOPMENT OF BIFUNCTIONAL OXYGEN ELECTRODE
TASKS I AND II. Final Report

M. Klein and S. Viswanathan

December 1986

APPLIED SCIENCE DIVISION

Prepared for the U.S. Department of Energy under Contract DE-AC03-76SF00098

DISCLAIMER

LBL-22661

ZINC/AIR BATTERY R & D
RESEARCH AND DEVELOPMENT OF BIFUNCTIONAL OXYGEN ELECTRODE
TASKS I AND II

Final Report

December 1986

by

M. Klein and S. Viswanathan

Energy Research Corporation
3 Great Pasture Road
Danbury, Connecticut 06810

for

Technology Base Research Project
Lawrence Berkeley Laboratory
University of California
Berkeley, California 94720

This work was supported by the Assistant Secretary for Conservation and Renewable Energy, Office of Energy Storage and Distribution of the U.S. Department of Energy under Contract No. DE-AC03-76SF00098, Subcontract No. 4528010 with the Lawrence Berkeley Laboratory.

ABSTRACT

Studies were conducted at ERC of the bifunctional oxygen electrode, specifically, research efforts were directed toward developing a relatively inexpensive air electrode that can function effectively both in the oxygen reduction and evolution modes.

The development of a rechargeable metal-oxygen (air) cell has been hampered to a great extent by the lack of a stable and cost effective oxygen electrode capable of use during both charge and discharge.

The standard platinum fuel cell electrode, when charged and discharged repeatedly, results in rapid self-discharge and reduced cycle life of the metal anode due to platinum migration.

Two approaches were considered in this research effort: The first utilized a low loading gold catalyst for oxygen reduction in combination with a nickel layer for oxygen evolution; the second approach examined a catalyst of the complex metal oxide perovskite type for both oxygen reduction and evolution.

The first type of bifunctional electrode consists of two distinct catalytic layers. The oxygen reduction catalyst layer containing a supported gold catalyst is in contact with a hydrophilic nickel layer in which evolution of oxygen takes place. Loadings of gold from 0.5 to 1.0 mg/cm^2 were investigated; carbon, graphite, metal and spinel oxides were evaluated as substrates.

The second part of the research effort was centered on developing a reversible oxygen electrode containing only one catalytic layer for both reduction and evolution of oxygen. The work was directed specifically to the study of perovskite type of oxides with the composition AA^1BO_3 where A is an element of the Lanthanide series, A^1 is an alkaline earth metal and B, a first row transition element. A number of perovskites were prepared at different process conditions, using Nd and La in group A, Sr, Ba and Cr in A^1 and Ni, Co and Mn in B. Employing these perovskites, air electrodes were prepared and characterized.

Initial polarization data obtained in unscrubbed air gave a value of approximately 200 millivolts vs. Hg/HgO reference electrode at a current density of 50 ma/cm^2. Electrodes were made both by roll-bonding and by pelletizing techniques and tested for polarization and cycle life.

In addition to establishing electrochemical parameters for the oxides, this study also indicates the optimum process conditions for the manufacture of oxides and fabrication of electrodes.

TABLE OF CONTENTS

LIST OF FIGURES

LIST OF FIGURES

LIST OF TABLES

EXECUTIVE SUMMARY

The R & D Program "Research & Development of Bifunctional Oxygen Electrodes" was completed in the third quarter of 1985. All the three tasks were brought to a successful termination; however, due to expiration of contract, life tests of certain promising electrodes could not be carried to completion.

By means of quarterly and summary reports, technical data and results of the research effort have been transmitted to LBL at specified intervals. The accomplishments are very significant, especially considering the duration and funding level of the program and warrants continued efforts.

The research efforts supported by experimental data demonstrated that bifunctional electrodes can be fabricated without using noble metal catalysts or carbon substrates and exhibit stable polarization over extended periods of time on all three regimes of operation - bifunctional, anodic and cathodic.

As a direct result of this research effort, a technical paper was presented at the 20th IECEC and the 7th Battery and Electrochemical Contractors' Conference. The article was published in the IECEC proceedings.

1.0 INTRODUCTION

Even though the major thrust of this research effort was the study of perovskite catalyst, limited efforts (Task I) were expended to investigate the O_2 reduction capabilities of electrodes with gold at a low loading. Results obtained with gold catalyzed electrodes were used as the basis for comparing the performance of electrodes prepared using perovskites as catalysts.

Under Task I, both commercially available gold powder and material prepared in-house were evaluated. In addition, materials other than carbon were investigated as substrates and catalyst supports.

Task II:

A systematic investigation was carried out to correlate the performance of the perovskite electrode for oxygen reduction with the conditions employed for synthesizing the compounds. Most of the electrodes had incorporated in them a separate hydrophilic nickel layer for oxygen evolution.

The transition metal oxides with substituted perovskitic structure were chosen to study the electrocatalytic activities for oxygen reduction. Typically, the catalyst was of the composition, $A_{1-x}\ A^1_x\ BO_3$

where:

A = element of the Lanthanide series, e.g. La

A^1 = element of alkaline earth series, e.g. Sr

B = first row transition metal e.g. Ni

The addition of the A^1 ion to the normal ABO_3 structure is considered necessary to provide sufficient conductivity for most of the compounds.

Task III:

An engineering analysis of the zinc air system for electric vehicles was performed. Several possible operating schemes were analyzed with regard to performance, system problems and cost-effectiveness and a separate report was submitted to LBL.

2.0 ELECTRODE PREPARATION

The electrodes consisted essentially of a multilayer composite structure of a porous polytetrafluoroethylene film, a hydrophobic catalytic layer for oxygen reduction, a hydrophilic nickel layer for oxygen evolution and a metal grid for current collection to produce gas-permeable and electrolyte repellant conductive electrodes. The two layers were produced by the practiced technique of roll-bonding after which the filler material was driven off and the layer sintered.

Two approaches were employed for the preparation of electrodes from perovskites. The first approach was to prepare a roll-bonded electrode similar to conventional fuel cell type electrodes; the only difference being the replacement of the noble metal catalyst in the oxygen reduction layer (Table 1) by perovskite.

The second method of preparation of the electrode utilized a pellet for the oxygen reduction layer. The required quantity of perovskite was mixed with Teflon powder and pressed at room temperature to a pellet, 1" in diameter. The pellet was then pressed onto the porous film, current collector and nickel layer to form a composite electrode. Both methods utilized a separate nickel layer for O_2 evolution.

In addition to the electrodes described above, a number of experimental electrodes were prepared with perovskites containing graphite to investigate if its addition would improve performance by increasing conductivity and active sites for electrocatalysis.

The various sequences in the preparation of the composite electrodes and their configurations are schematically shown in Figures 1 and 2.

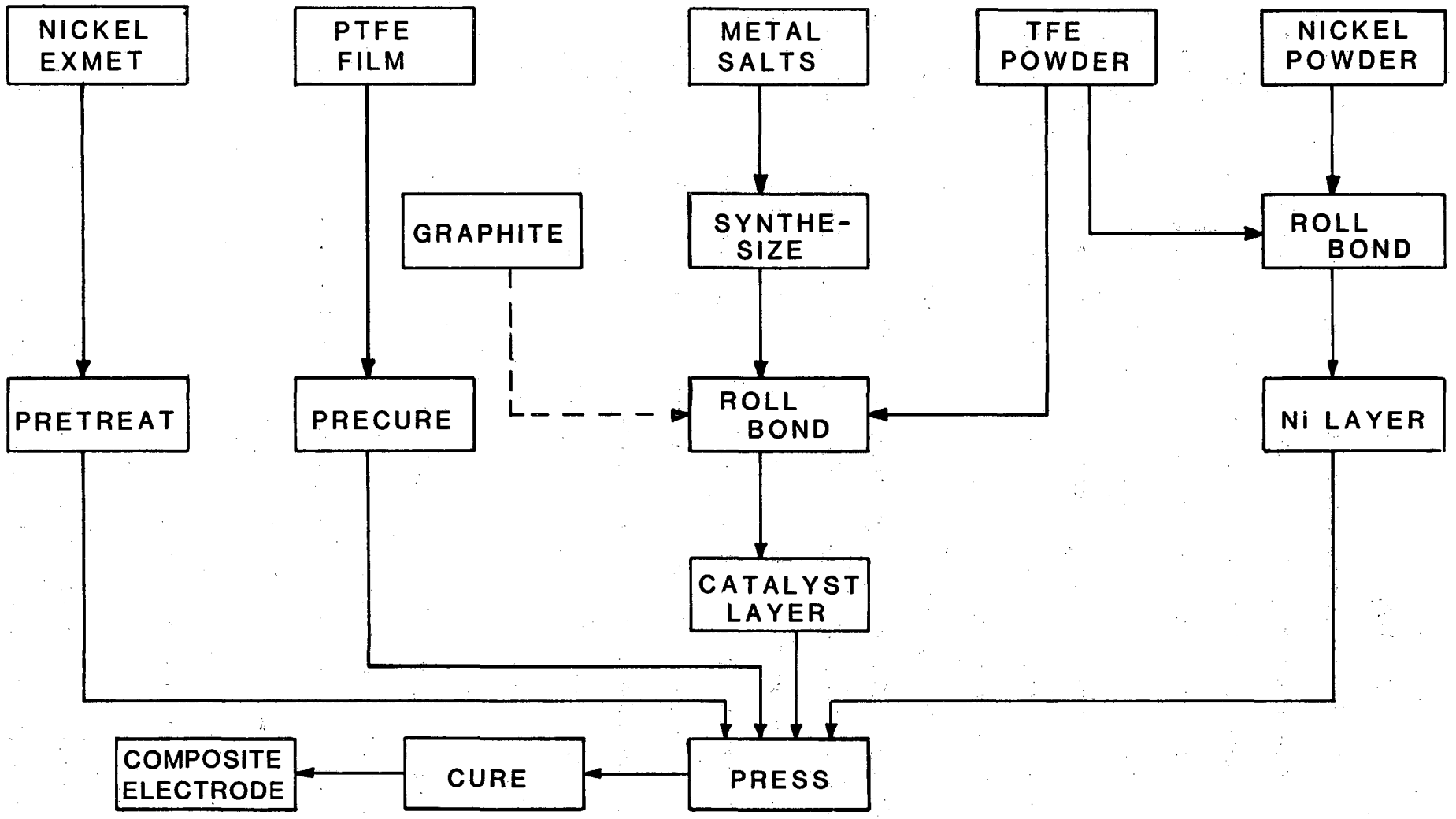

FABRICATION OF COMPOSITE ELECTRODE

FIGURE 1

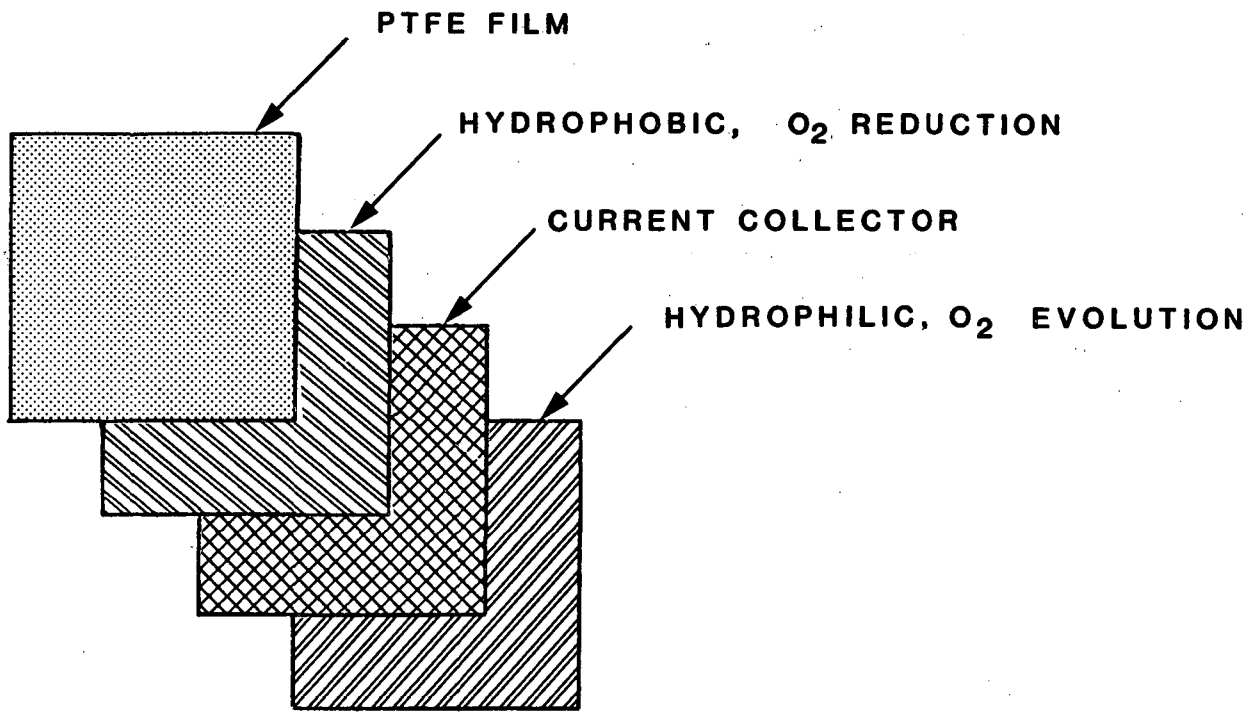

COMPOSITE MULTILAYERED ELECTRODE STRUCTURE

FIGURE 2

TABLE 1

ELECTRODE CONFIGURATION

Porous Film	PTFE, Chemplast, Precured
Current Collector	Ni Exmet, 7 Ni 4/0, FEP Processed
O_2 Reduction Layer	Perovskite 60 mg/cm², Teflon 25% Substrate
O_2 Evolution Layer	Ni 287, Teflon 5%
Roll-Bonding	
-Solvent	Shellsol
-Binder	Teflon
-Filler	Ammonium Bicarbonate

3.0 ELECTRODE TESTING

Electrodes were tested in a half-cell made of plexiglass using a nickel screen as the counter electrode. Potentials of the test (air) electrodes were measured against a mercury-mercuric oxide reference electrode both during charge and discharge cycles.

Polarization tests were conducted both in ambient air and in pure oxygen at current densities of up to 100 mA/cm^2. This was followed by cycling the electrodes on a regime of charge 1 hour at 10mA/cm^2 and discharge for 1 hour at 20 mA/cm^2.

Initially the electrodes were cycled in atmospheric air. This led to rapid degradation due to carbonation resulting in high values of polarization. Test conditions were modified to monitor the electrode in an atmosphere of pure oxygen during cycling. This has resulted in preventing deterioration of the electrodes and in obtaining lower polarizations.

In addition to alternate charge-discharge cycling regime, two additional series of tests were done to evaluate the electrodes. Electrode performance was monitored under conditions of continuous discharge (cathodic, O_2 reduction) and continuous charge (anodic, O_2 evolution) in order to compare the potentials with the values obtained under cycling conditions. All the tests were carried out in an atmosphere of pure oxygen.

4.0 EXPERIMENTAL RESULTS

4.1 Task I - Bifunctional gold electrode.

4.1.1 Preparation of catalyst and substrate

The following types of gold powder were evaluated as catalysts:

1. Amorphous gold powder, Metz metallurgical Corp., Product # 653, 14-18 g/in^3, -3 to -5 microns, 3 to 6 m^2/g.
2. Gold chloride reduced by Mg powder in presence of Hg @ 10°C.
3. Gold chloride (in KOH) reduced by hydrazine @ 54°C.

The powders were not characterized separately; however, as active material of the O_2 electrode, no differences in performance were noticeable.

Darco carbon G-60, Lonza graphite KS-44, NiB, SnO_2, Al_2O_3 and cobalt spinels of Ni, Co, Cd, Mg and Mn were investigated as substrate materials. The materials were mixed to the catalyst both by admixing and co-precipitation techniques.

From the materials thus prepared, electrodes were fabricated and tested as specified earlier (see 2.0 and 3.0). Only the roll-bonding method was used for preparing electrodes.

Polarization tests were conducted in air and pure oxygen up to 100 mA/cm^2 after which each electrode was cycled on an automatic cycler on the regime -- charge 4 hours at 10mA/cm^2, discharge 4 hours at 20 mA/cm^2. Cycling was terminated when two successive voltages at the end of discharge were greater than 1.0 V. All cycling was carried out on an atmosphere of ambient air.

4.1.2 SUMMARY OF RESULTS

- Discharge potential at 20mA/cm^2 is independent of charge current densities between 5 and 20 mA/cm^2. However, end

of charge potentials are dependent on charge currents.

- Without the PTFE backing film, charge and discharge potentials show lower polarization by approximately 120 and 60 millivolts respectively, but electrodes without film deteriorated rapidly and started weeping.

- Polarization values showed a vast improvement (especially) at higher current densities) when tested in pure oxygen, compared to unscrubbed air, (Figures 3 and 4). Based on this, the electrodes are expected to perform much better if cycled in an atmosphere of scrubbed air or pure oxygen.

- At low loadings of Gold (0.5-0.7 mg/cm^2) no difference in performance was noticeable between gold purchased commerically and those prepared in-house.

- The stabilizing effect of the catalytic layer for oxygen reduction is demonstrated in Figure 5.

- The importance of catalytic layer and cathode configuration are shown in Figure 6.

- Four successive tests of one electrode of the composition #BG x-3 showed initial polarization values of 187, 178, 174 and 194 millivolts at 20 mA/cm^2. This compares favorably with a value of 200 millivolts obtained with the control Pt electrode. However, the former deteriorated rapidly on cycling.

- Catalyst and/or supports prepared by co-precipitation techniques did not improve performance over admixing matrials.

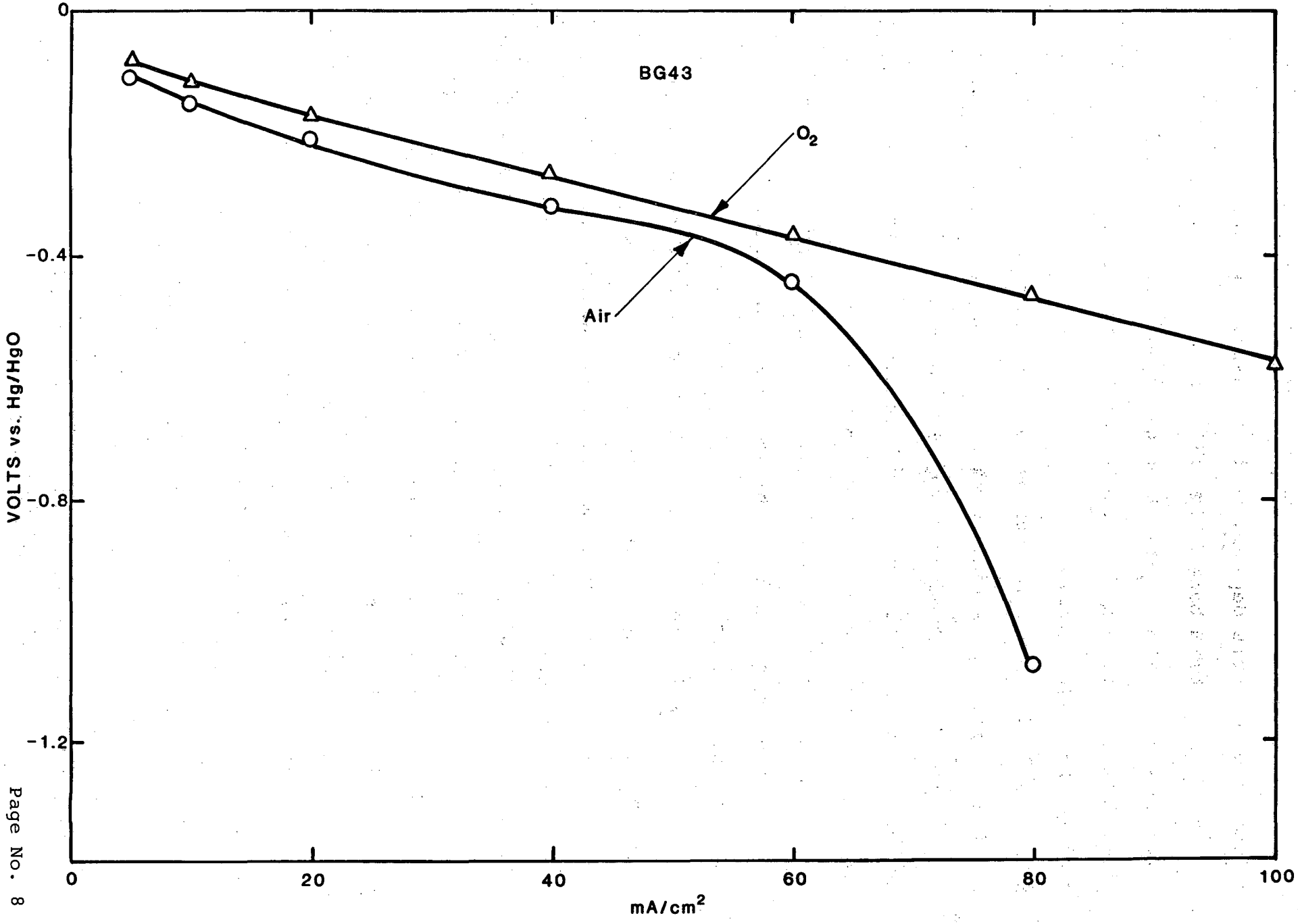

FIGURE. 3 E-1 CURVE FOR BG43

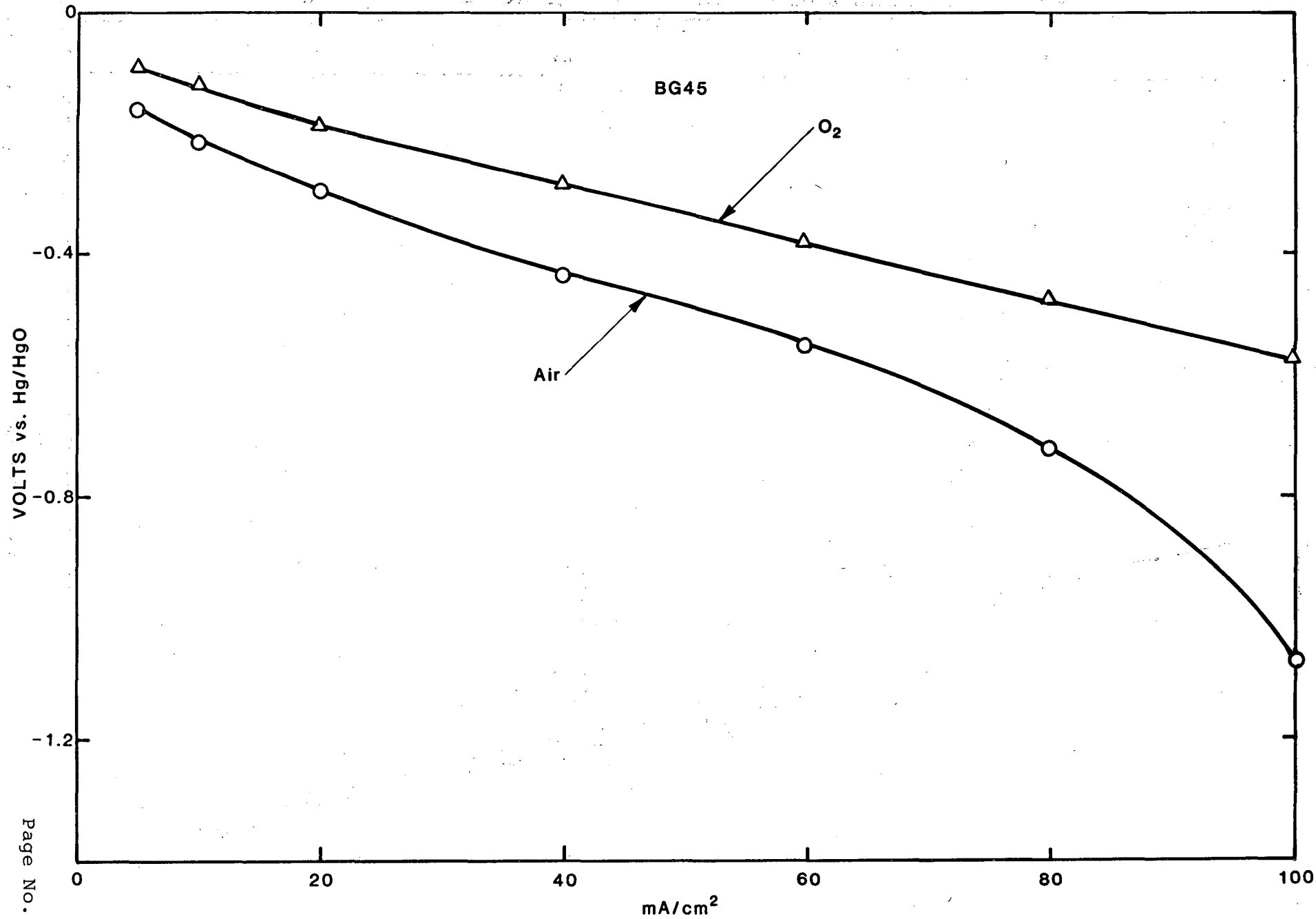

FIGURE. 4 CURVE FOR BG45

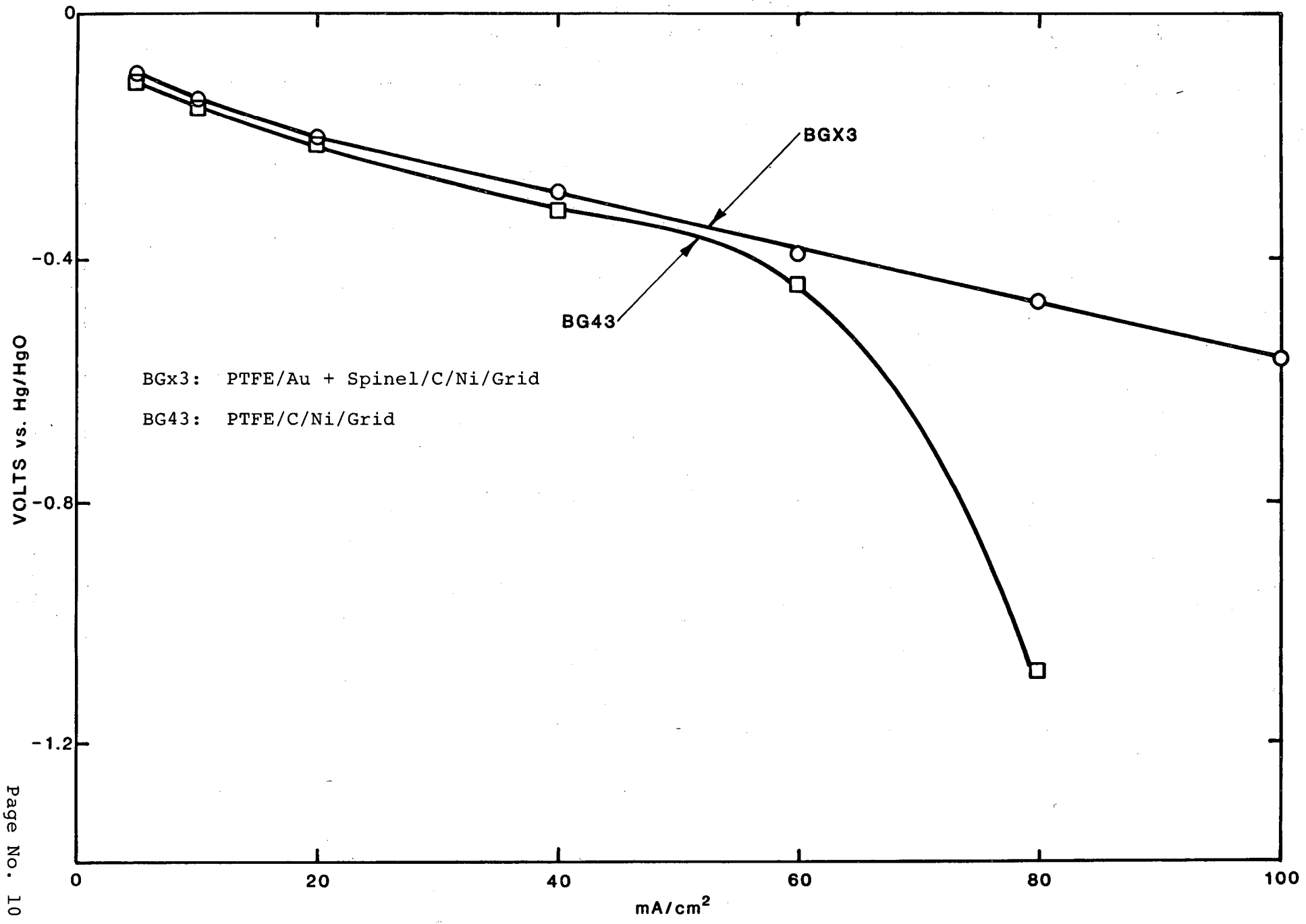

FIGURE. 5 COMPARISON OF ELECTRODES WITH & WITHOUT CATALYST

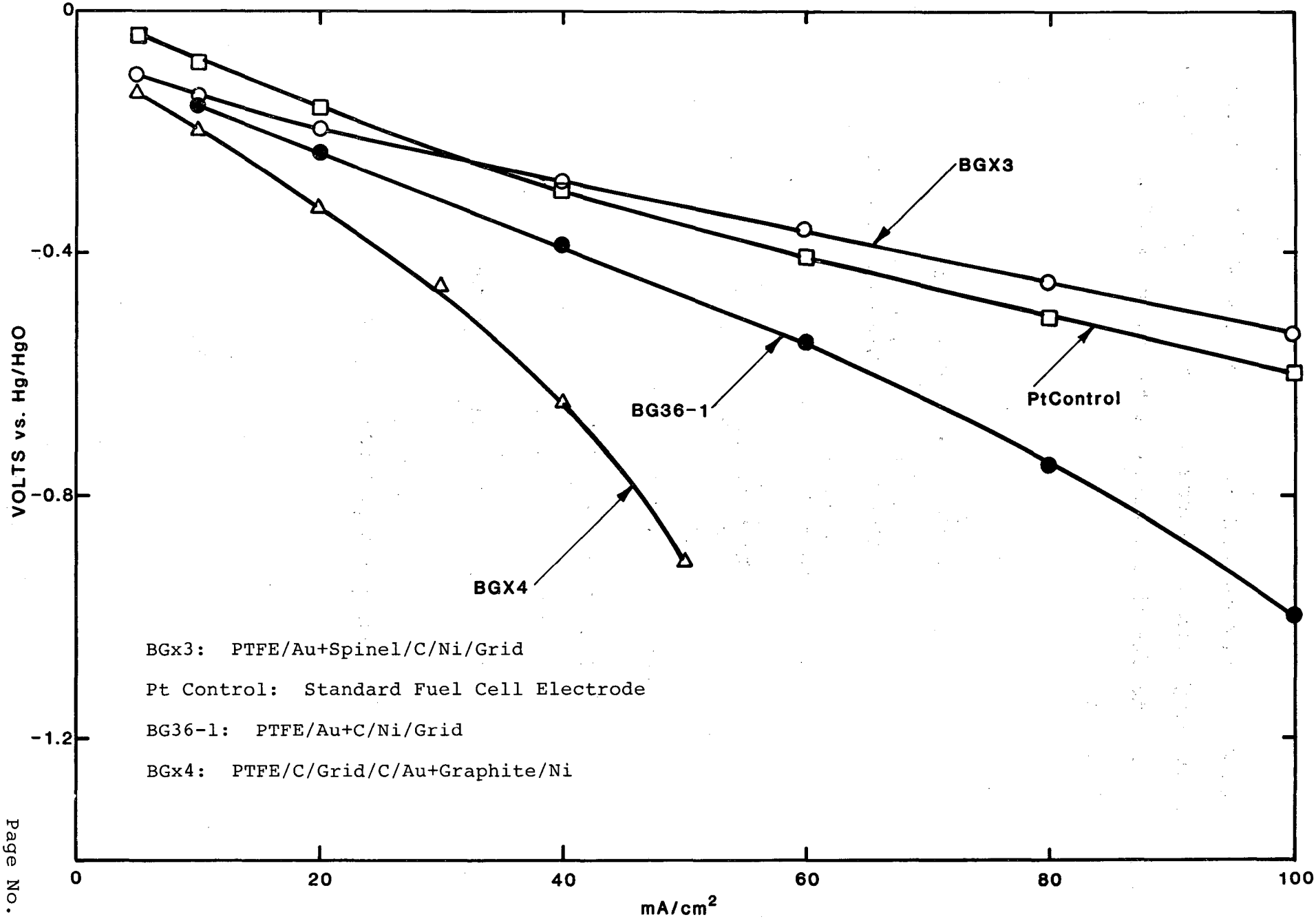

FIGURE. 6 COMPARISON OF ELECTRODE PERFORMANCE

Over 30 different electrodes were evaluated. In addition to employing different substrates, electrodes with differing configurations were fabricated, selected examples of which are as follows:

BG x 3	Au+ PTFE/Cd Spinel/G 60/Ni/Grid
x 4	G 60 Au+ PTFE/Film/Grid/G 60/Graphite/Ni
25	Au+ PTFE/Graphite/Ni/Grid
26-1	Au+ PTFE/Co Spinel/Ni/Grid PPTD on graphite
26-2	26-1 Without PTFE
36	Au+ PTFE/G 60/Ni/Grid
43	PTFE/G 60/Ni/Grid
45	Au+ PTFE/Ni Spinel/G 60/Ni/Grid

TABLE 2

ELECTRODE CONFIGURATION

As can be seen from Table 3, the most promising catalyst support is graphite. Carbon is good initially but deteriorates on cycling. Metal and spinel oxides show stable though high values of polarization, probably due to high resistivity.

	Polarization	
	Initial	On Cycling
Carbon G 60	High After 50 mA/cm²	High
G 60 + Gold	Low	High
Graphite + Gold	Medium	Medium
Metal Oxide + Gold	High	High
Spinels + Gold	High	High

TABLE 3

COMPARISON OF SUBSTRATES

4.1. Transport Hindrance

Polarization data were measured on electrodes BG43 and BG45 both in atmospheric air and pure oxygen. The electrodes had the following configurations:

BG43 - PTFE/G60/Ni Layer/grid layer

BG45 - PTFE/Au + Ni Spinel/G60/Ni Layer/Grid
Layer Layer

Electrode BG43, which did not contain gold, polarized rapidly at current densities greater than 50 mA/cm², when measured in air. Presence of gold in electrode BG45 resulted in moderating the polarization even at higher current densities up to 100 mA/cm².

The polarization in air and oxygen for electrodes BG43 and BG45 is shown in Figures 7 and 8. The efficiency factor of a particular electrode operating with air and pure oxygen can be compared at the same current density:

$$I = (E_{air}) = I(E_{O_2})$$

Under these conditions the potentials in air and oxygen will differ:

$$E_{air}\ (I) \neq E_{O_2}\ (I)$$

At sufficiently low current densities the transport hindrances are minimal so that the value of ΔE, $(E_{O_2} - E_{air})$ should be independent of the current density.

With increase in current density, efficiencies decrease both in air and oxygen. The electrode operating in air will decrease more rapidly than one operating in oxygen and the effect will be more pronounced at higher current densities. Accordingly, increase in current density causes an increase in the value of ΔE.

It should be mentioned that the values of ΔE are free of IR drop in the electrolyte between air and reference electrodes.

Experimental E-I curves are shown in Figures 7 and 8. It can readily be seen that the value of ΔE is independent of I at current densities between 10 and 60 mA/cm^2 for electrode BG43 and between 10 and 80 mA/cm^2 for electrode BG45. Since the former did not contain any gold, it polarized readily in air at higher currents -- a phenomenon that is reflected in the values of ΔE which show a corresponding increase.

Comparison of the ΔE-I curves of different electrodes could be used to estimate the transport hindrance in air electrodes. This is illustrated in Figure 9 for the two electrodes.

4.2 Task II - PEROVSKITE ELECTRODE

4.2.1 Perovskite Preparation

The perovskites were prepared by the decomposition of nitrates, acetates, oxalates or carbonates of the respective elements. The appropriate amount of each reagent was mixed in the calculated stoichiometric proportions and evaporated to dryness with simultaneous mechanical mixing. The residue was

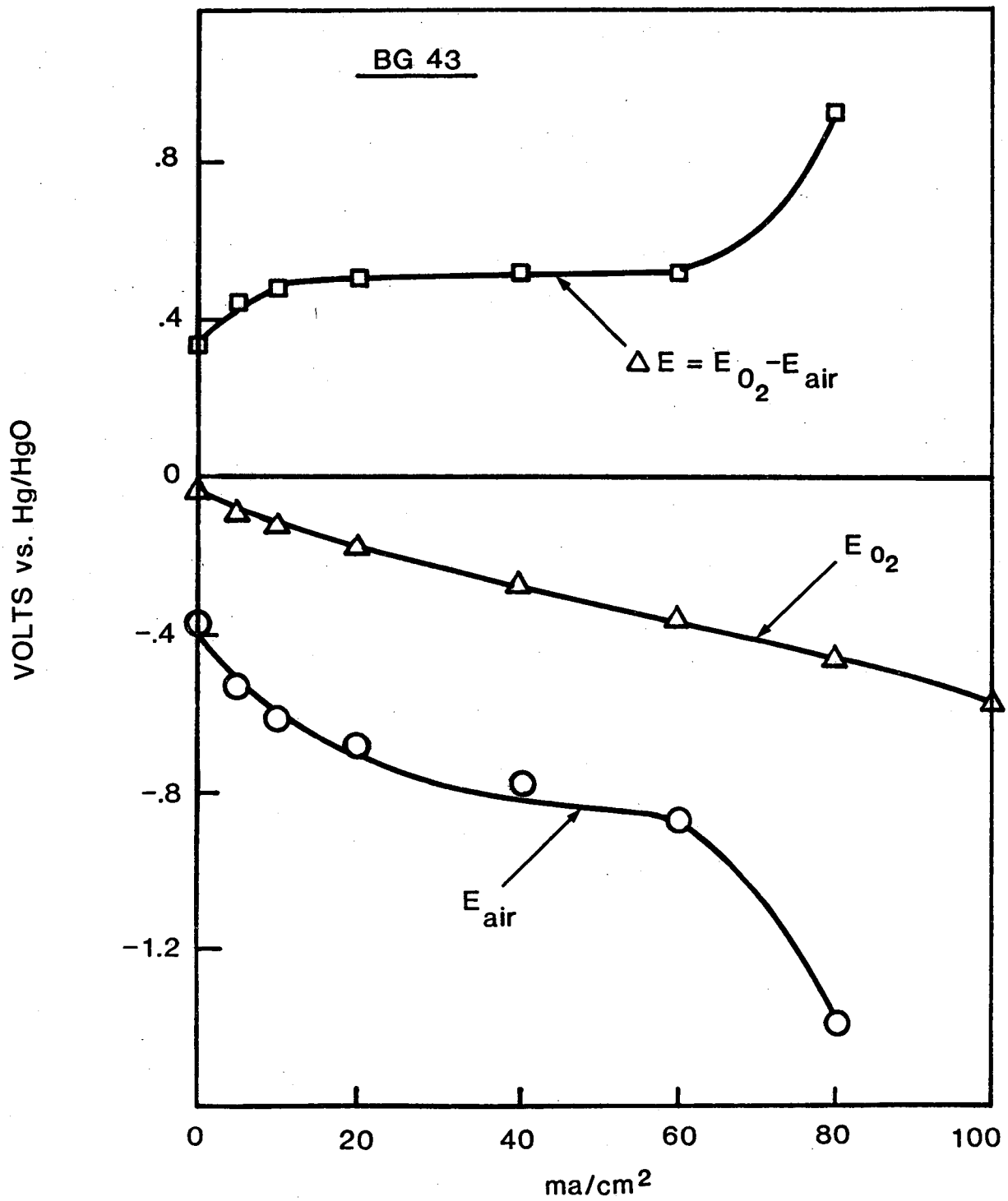

POLARIZATION CURVES FOR O_2 REDUCTION
ELECTRODE #BG 43

FIGURE 7

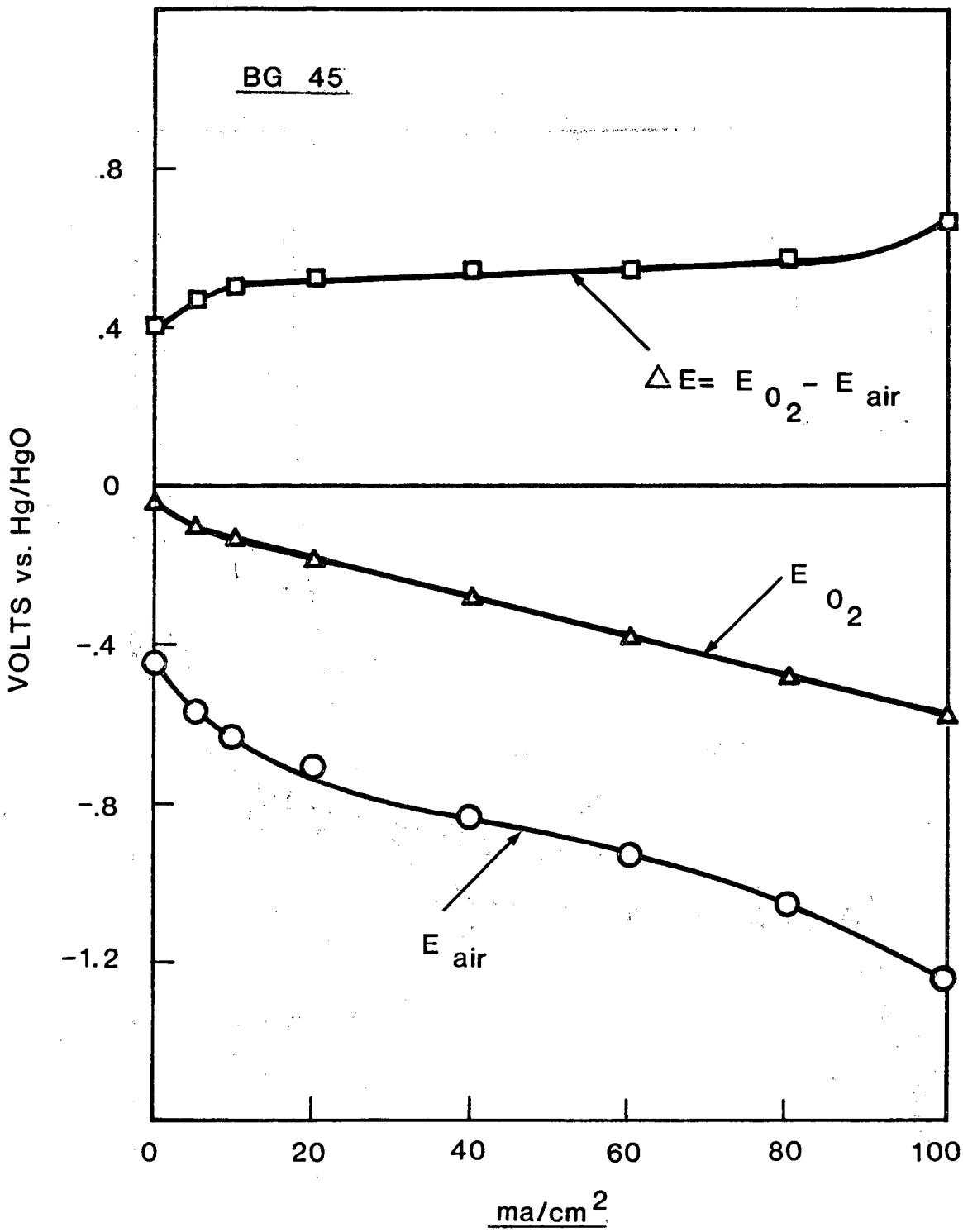

POLARIZATION CURVES FOR O_2 REDUCTION
ELECTRODE #B 45

FIGURE 8

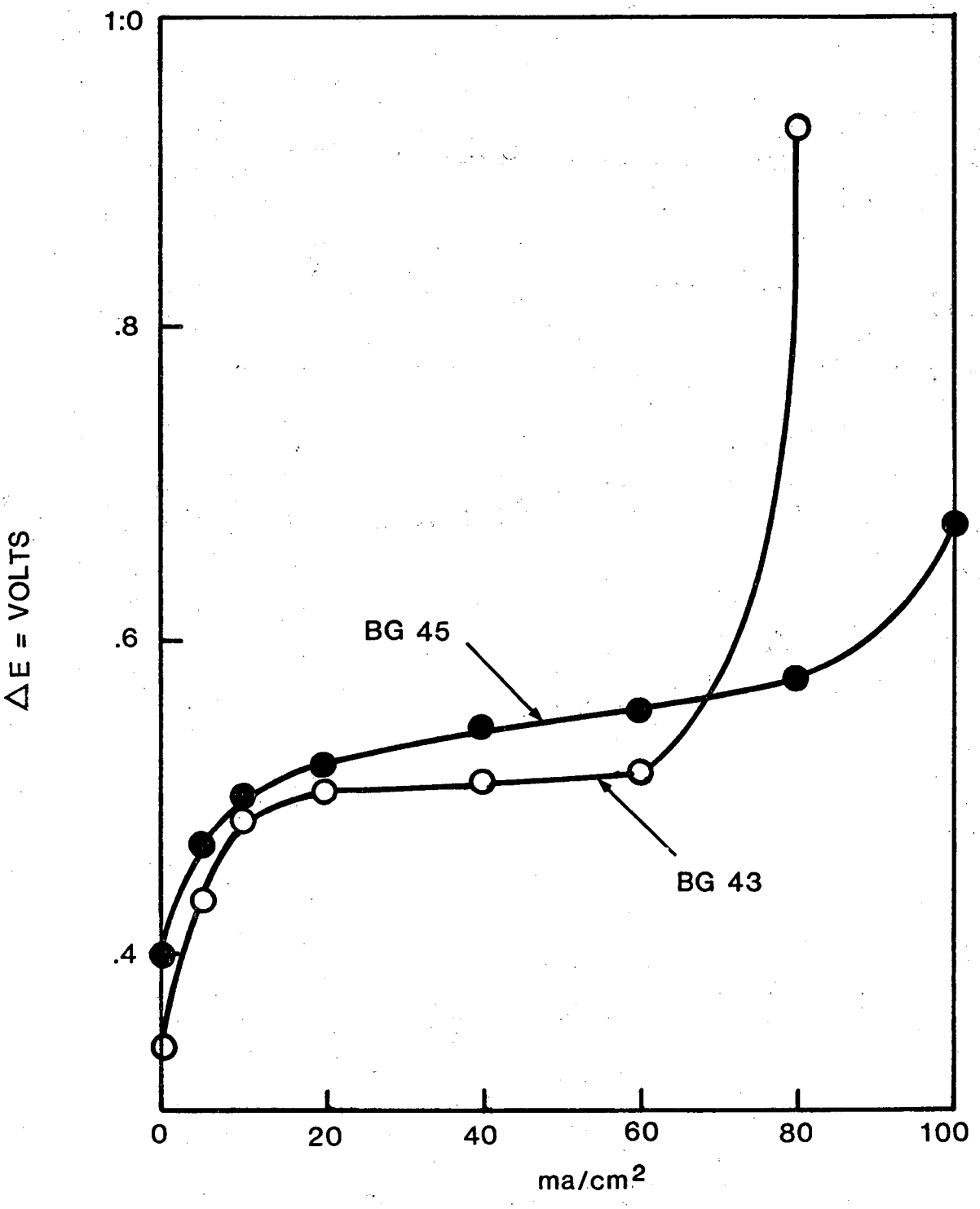

COMPARISON OF TRANSPORT HINDRANCE

FIGURE 9

scraped, ground and again mixed thoroughly by hand. The uniformly mixed powder was then placed in an alumina crucible and fired in a furnace. The sintering time and temperatures were varied between 4 and 72 hours and 600 and 950°C respectively. No controlled atmospheric conditions were employed and all sintering operations were carried out in an atmosphere of ambient air.

At the completion of sintering, the perovskite was removed from the furnace, cooled, ground and stored in a closed container. The conductivity of the perovskites was measured and selected samples were sent to St. Joe Technical Center for x-ray diffraction analysis which showed perfect match to patterns of known phases. Energy dispersive x-ray analysis confirmed that the bulk composition of material was identical to formulation and crystal structure was found to be cubic or rhombic.

The starting chemicals and process conditions used in the preparation of the various perovskites are summarized in Table 4 and the resistivities in Table 5.

TABLE 4a

PEROVSKITE PREPARATION

S #	I.D. #	COMPOSITION	STARTING MATERIAL	CONDITION	
				HRS	°0
1	P1-2	$Nd_{.8}Sr_{.2}Co_{.9}Ni_{.1}O_3$	acetates	5	900
2	P3-A	$La_{.8}Sr_{.2}Co_{.9}Ni_{.1}O_3$ + graphite	"	"	"
3	P3-B	"	"	16	"
4	P4-4	$La_{.8}Sr_{.2}Co_{.9}Ni_{.1}O_3$	"	5	"
5	P4-B	"	"	16	"
6	P5-A	$La_{.5}Sr_{.5}CoC_3$	"	5	"
7	P5-B,C	"	"	16	"
8	P6	$LaMnO_3$	nitrates	27	950
9	P7	$LaNiO_3$	"	16	600
10	P8	"	"	48	800
11	P9	"	oxalates pptd. with NaOH	18	850
12	P10	"	oxalates	"	"
14	P20	$Nd_{.8}Sr_{.2}Co_{.9}Ni_{.1}O_3$	acetates	16	900
15	P21	$La_{.5}Sr_{.5}MnO_3$	nitrates	"	"
16	P22	$La_{.5}Sr_{.5}BaO_3$	"	"	"
17	P23	$LaCrO_3$	oxides	23	"
18	P24	$La_{.5}Sr_{.5}CoO_3$	nitrates	24	"
19	P25	"	"	40	"
20	P27	$LaNiO_3$	nitrates	46	900
21	P28	"	"	70	"
22	P30	$La_{.5}Sr_{.5}CoO_3$	acetates	16	"
23	P31	$Nd_{.5}Sr_{.5}CoO_3$	"	4	"
24	P32	$Nd_{.8}Sr_{.2}Co_{.9}Ni_{.1}O_3$	"	5	"
25	P33	$LaNiO_3$	nitrates	16	800
26	P34	"	"	48	850
27	P36	$LaRuO_3$	La_3O_3, RuO_3, Ru	24	900

TABLE 4a - continued

PEROVSKITE PREPARATION

S #	I.D. #	COMPOSITION	CONDITION	
			HRS	°0
28	P35	$La_{.5}Sr_{.5}Co\ O_3$	16	900
29	P40	$SrRuO_3$	48	"
30	P41	$La_{.5}Sr_{.5}Ru\ O_3$	24	"
31	P42	$La_{.75}Sr_{.25}Co\ O_3$	16	"
32	P43	"	"	"
33	P44	$NdNiO_3$		
34	P45	$La_{.5}Sr_{.5}Co\ O_3$	16	"
35	P46	$La_{.9}Bi_{.1}Ni\ O_3$	17	925
36	P47	$La_{.5}Ru_{.5}Co\ O_3$	"	900
37	P48	$La_{.5}Sr_{.5}Co\ O_3$	18	"
38	P49	$La_{.5}Sr_{.5}Ru\ O_3$	24	"
39	P50	$La_{.5}Sr_{.5}Co\ O_3$	"	"
40	P50-S	$La_{.5}Sr_{.5}Co\ O_3 + H_2S$ (excess)	"	"
41	P51	$Nd_{.5}Sr_{.5}Co\ O_3$	4	900

TABLE 4b

PEROVSKITE PREPARATION

S #	I.D. #	COMPOSITION	STARTING MATERIAL	CONDITION	
				HRS	°0
1	P53	$LaRuO_3$	La_2O_3, RuO_2, Ru	24	900
		$SrRuO_3$	SrO, RuO_2	48	900
		$La_{.5}Sr_{.5}CoO_3$	Acetates		
		$La_{.5}Sr_{.5}Ru_{.5}CO_{.5}O_3$		16	900
2	P54	$La_{.9}Nd_{.1}NiO_3$	Nitrates Acetates	24	950
3	P56	$LaCoO_3$	Nitrates	24	900
4	P57	$NdCoO_3$	Acetates	24	900
5	P58	$La_{.8}K_{.2}MnO_3$	Nitrates	24	900
6	P61	$Nd_{.4}La_{.4}Sr_{.2}Co_{.9}Ni_{.1}O_3$	Nitrates, Acetates	24	900
7	P62	$La_{.95}Zr_{.05}CoO_3$	Nitrates, ZrO_2	24	900
8	P50A	$La_{.5}Sr_{.5}CoO_3$	Acetates	8	900
9	P50B	"	"	16	900
10	P50C	"	"	48	900

TABLE 5a

RESISTIVITY OF PEROVSKITES

@ 25°C

S. No.	ID No.	PEROVSKITE	OHM	OHM·CM
1	P1	$Nd_{.8}Sr_{.2}Co_{.9}Ni_{.1}O_3$	231	33
2	P4	$La_{.8}Sr_{.2}Co_{.9}Ni_{.1}O_3$	185	27
3	P5	$La_{.5}Sr_{.5}CoO_3$	25	-
4	P6	$LaMnO_3$	111,000	-
5	P8	$LaNiO_3$	20	4
6	P20	$Nd_{.8}Sr_{.2}Co_{.9}Ni_{.1}O_3$	550	-
7	P21	$La_{.5}Sr_{.5}MnO_3$	106	-
8	P22	$La_{.5}Ba_{.5}MnO_3$	2,240	312
9	P23	$LaCrO_3$	14,000	-
10	P24	$La_{.5}Sr_{.5}CrO_3$	46,000	-
11	P27	$LaNiO_3$	220	58
12	P30	$La_{.5}Sr_{.5}Co\ O_3$	40	9
13	P31	$Nd_{.5}Sr_{.5}Co\ O_3$	138	
14	P33	$LaNiO_3$	47	
15	P34	"	40	
16	P36	$LaRuO_3$	4.5	1.8

TABLE 5 b

RESISTIVITY OF PEROVSKITES @ 25°C

S #	I.D. #	COMPOSITION	OHM	OHM-CM
1	P53	$La_{.5}Sr_{.5}Ru_{.5}Co_{.5}O_3$	70	44
2	P54	$La_{.9}Nd_{.1}NiO_3$	18	10
3	P55	$LaCoO_3$	6500	1540
4	P57	$NdCoO_3$	Hl	Hl
5	P58	$La_{.8}K_{.2}MnO_3$	Hl	Hl
6	P61	$Nd_{.4}La_{.4}Sr_{.2}Co_{.9}Nl_{.1}O_3$	Hl	Hl
7	P62	$La_{.95}Zr_{.05}CoO_3$	Hl	Hl
8	P50A	$La_{.5}Sr_{.5}CoO_3$	32	12
9	P50B	"	154	33
10	P50C	"	120	29

4.2.2 EXPERIMENTAL RESULTS

Electrodes prepared by pressing the perovskites into pellets exhibited better conductivities and electrochemical charateristics, compared to roll-bonded electrodes. However, when subjected to life tests the pelletized electrodes failed prematurely. Examination of the electrodes revealed that the pellets developed cracks through which electrolyte permeated onto the Teflon film. The failure mechanism is therefore attributed to mechanical degradation and not to loss in catalytic activity.

Electrode fabrication by using the pelletized techniques was therefore discontinued and efforts were directed back to the roll-bonded method. The higher than desirable values of the resistivities of the perovskites resulted in rapid polarization of the electrodes when perovskites alone were used to form the catalytic layer. But when the perovskite was admixed with graphite, it was found that the conductivity improved substantially and polarization values remained in an acceptable range. In addition, the electrodes showed stable potentials on life tests both on a continuous cathodic mode and on anodic and cathodic cycling regimes. The improved characteristics are considered to result from improved conductivity and increased active sites for electrocatalysis provided by graphite.

Performance characteristics of two electrodes on continuous discharge at a current density of 20 mA/cm^2 are shown in Figure 10 Electrode containing $La_{.5}Sr_{.5}Co\ O_3$ to which graphite was

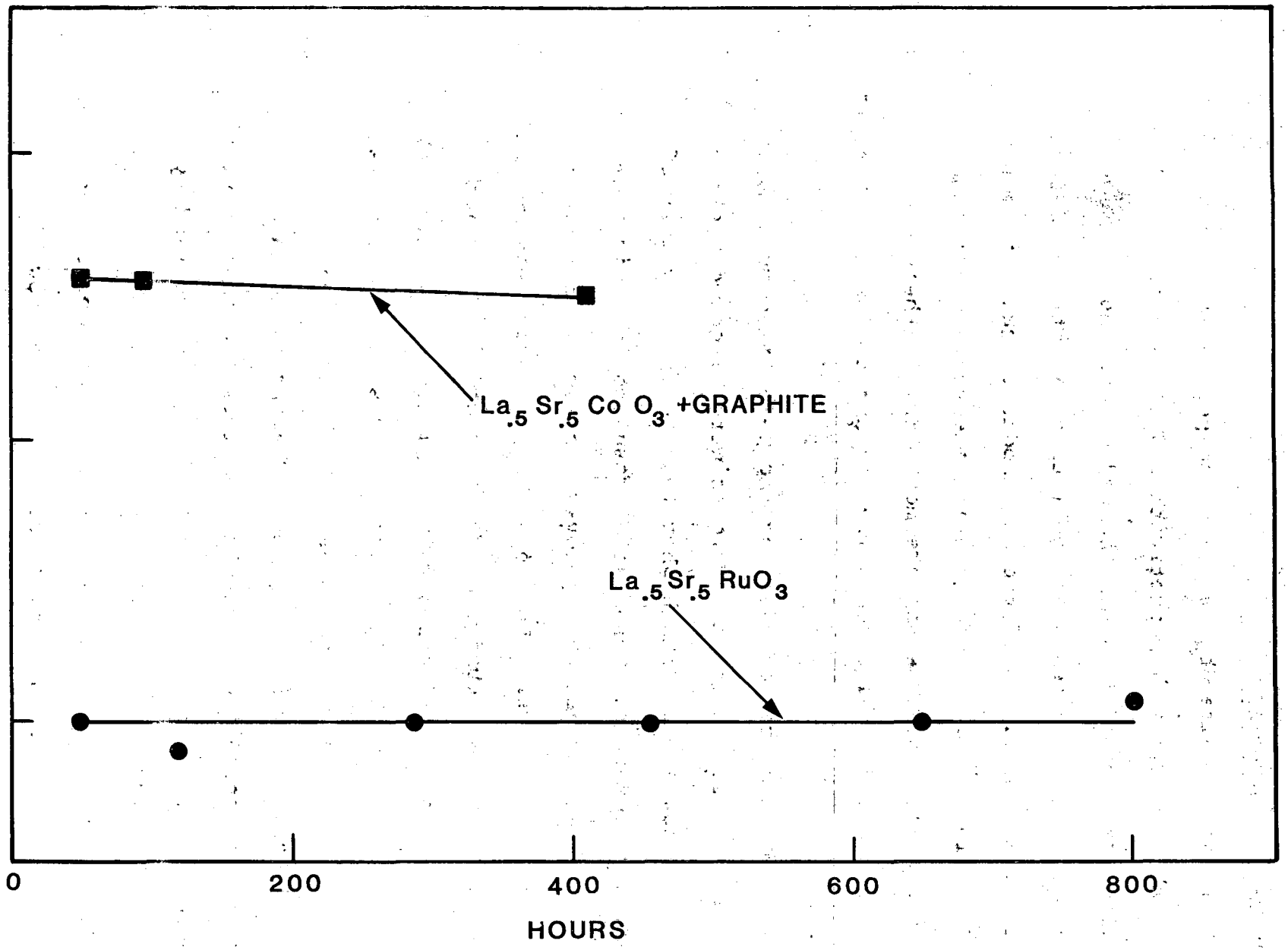

CONTINUOUS DISCHARGE IN O_2 @ 20 mA/cm^2

FIGURE 10

added shows a stable potential of approximately 200 millivolts after 400 hours of operation. Perovskite electrode prepared with $La_{.5}$ $Sr_{.5}$ Ru O_3 without graphite also exhibited a stable potential over 800 hours even through the magnitude was much higher. It is believed that addition of graphite would lower the polarization.

The normal loading of perovskites was in the order of 60-100 mg/cm² of electrode area. When graphite was added to the perovskites, the total loading was kept the same and the amount of perovskite was halved to give a weight ratio of graphite to perovskite of 1:1.

Experimental results of electrodes when tested on a cycling regime are shown in Figure 11. The test conditions were 4 hours, anodic @ 10 mA/cm² followed by 4 hours, cathodic @ 20 mA/cm². The cathodic potentials started at 400 millivolts and increased gradually to 600 millivolts after 90 cycles. The currents were then reduced to 5 mA/cm² and 10 mA/cm² for the anodic and cathodic modes respectively and cycling was continued. This modification resulted in reducing the polarization to a steady value of 380 millivolts for an additional 210 cycles. For purposes of comparison, a low loading bifunctional gold electrode was also tested simultaneously. The results are also shown in Figure 11.

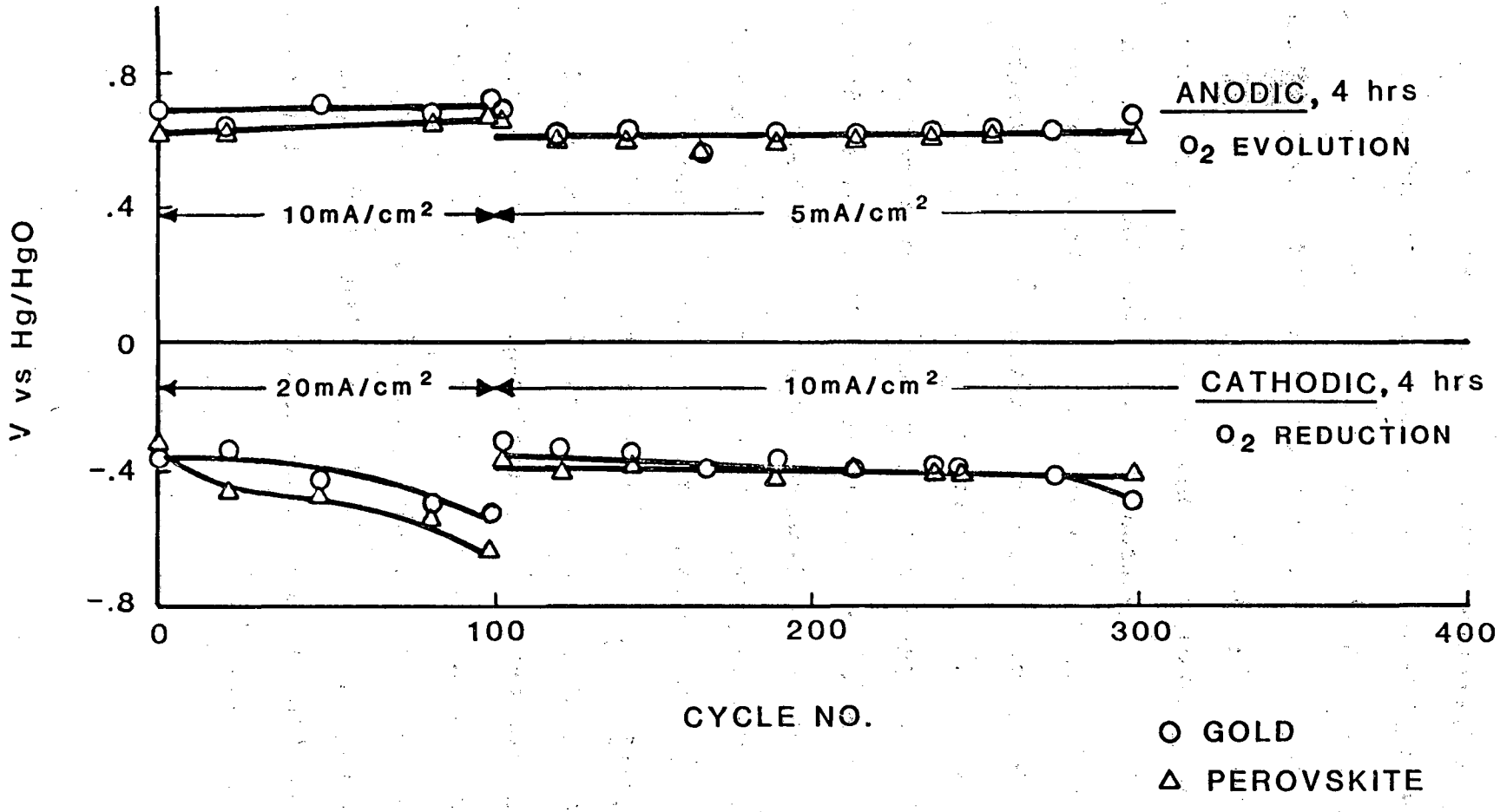

POLARIZATION ON CYCLING

FIGURE 11

The variation of potentials with time for cycles No. 7, 60 and 283 are shown in Figures 12, 13 and 14 for perovskite and gold electrodes. It can be readily seen that the potentials remain stable in both anodic and cathodic modes.

The polarization curves for O_2 reduction were obtained in an atmosphere of pure oxygen. The data for pelletized electrodes made with lanthanum and neodymium based perovskites are shown in Figure 15. As mentioned earlier, electrodes fabricated with $La_{.5}$ $Sr_{.5}$ Co O_3 catalyst pressed into a pellet exhibited the best performance.

Similar results are presented in Figure 16 for the roll-bonded electrodes. The results clearly indicate the necessity of admixing graphite to the perovskite, for this method of electrode fabrication.

4.2.3 ELECTRODE PERFORMANCE ON CYCLING

A number of electrodes were tested under alternate charge-discharge cycling conditions. The current densities during charge and discharge were kept at 10 and 20 mA/cm^2 respectively. In order to accelerate the cycling frequency, the total times were reduced from eight to two hours such that the duration of charge and discharge modes were one hour each. All tests were performed in an atmosphere of pure oxygen. Tests were terminated when the polarization values reached an arbitrarily set value of 500 millivolts against Hg/HgO reference electrode.

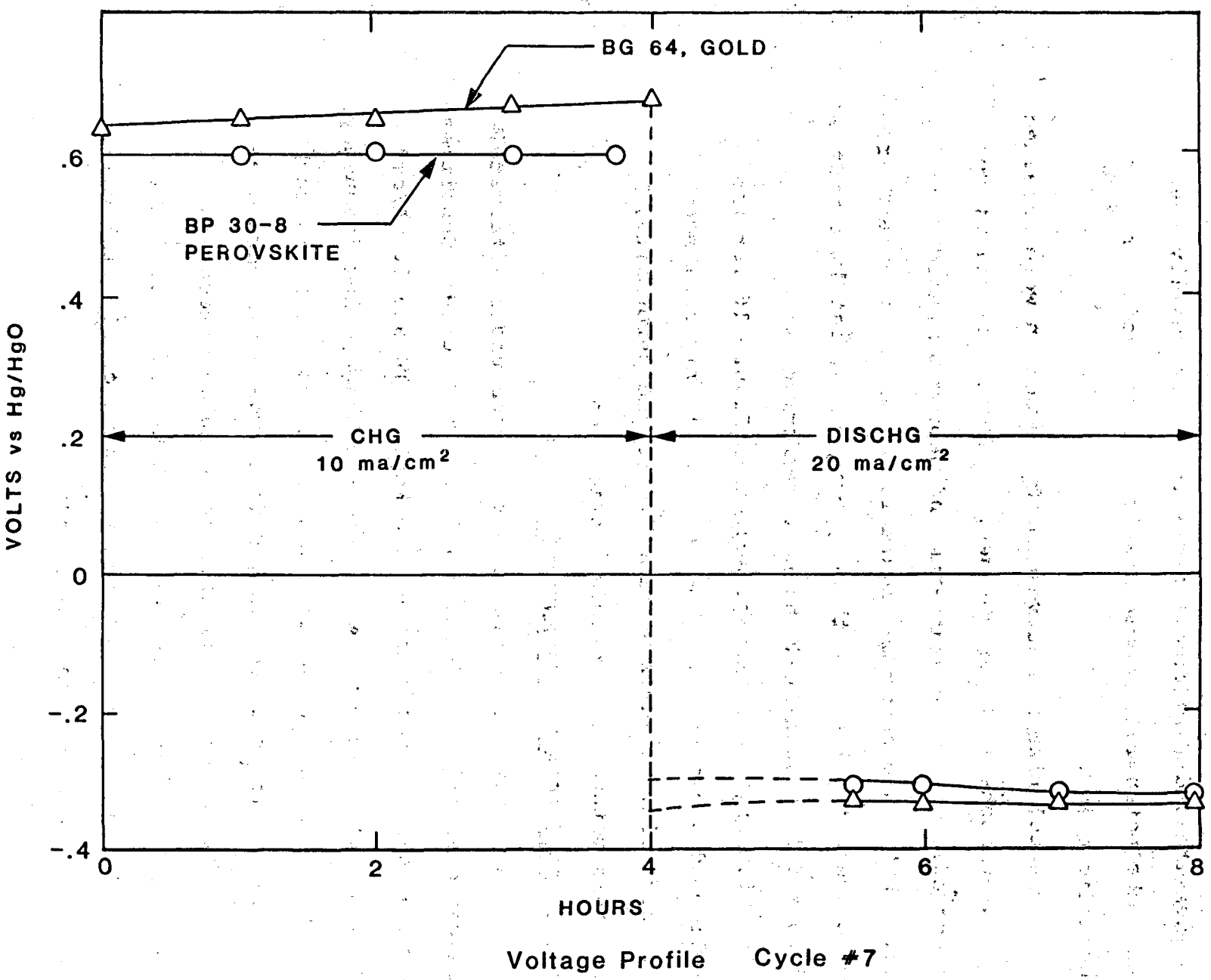

Voltage Profile Cycle #7

FIGURE 12

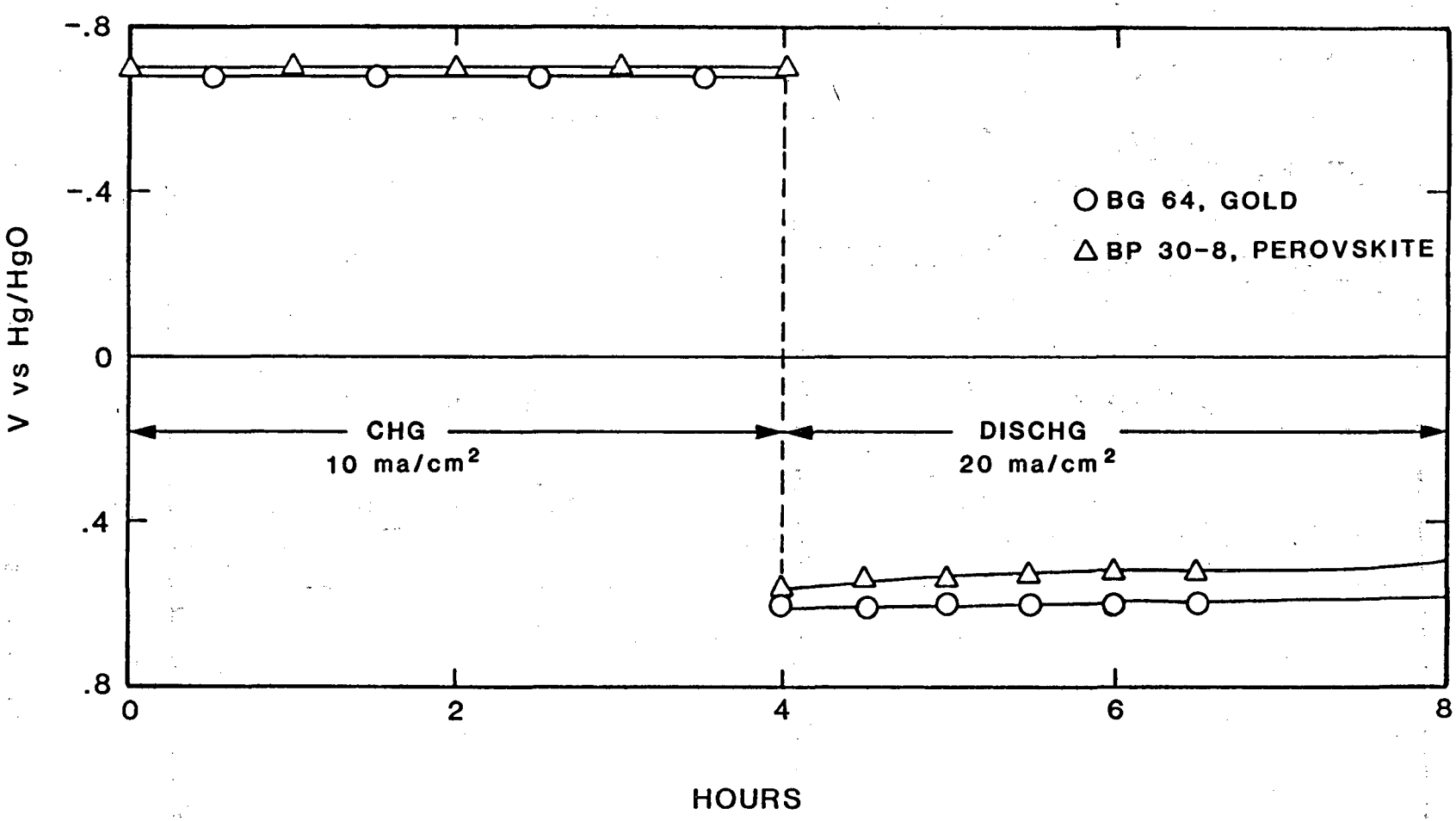

Voltage Profile Cycle # 60

FIGURE 13

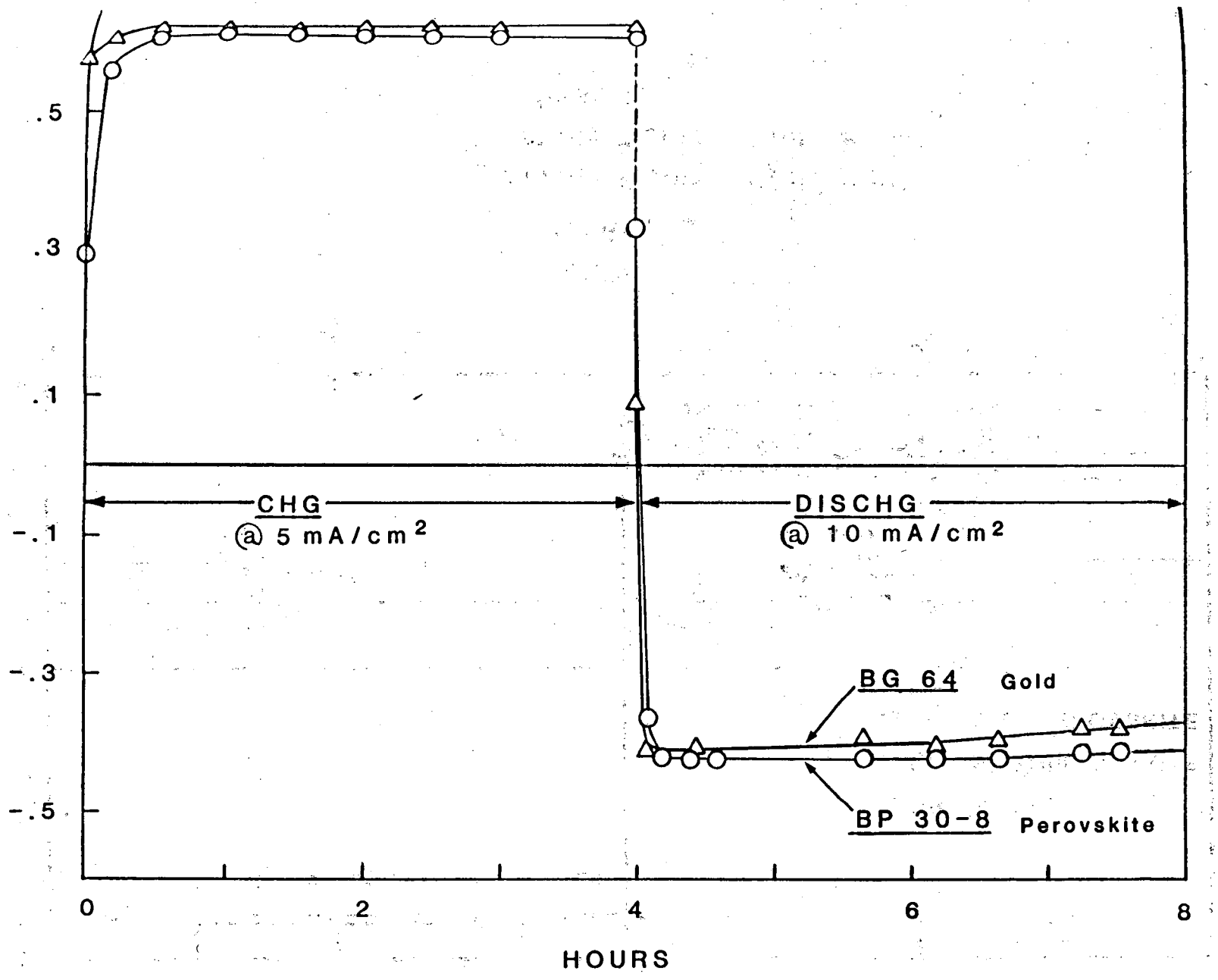

VOLTAGE PROFILE-CYCLE #283

FIGURE 14

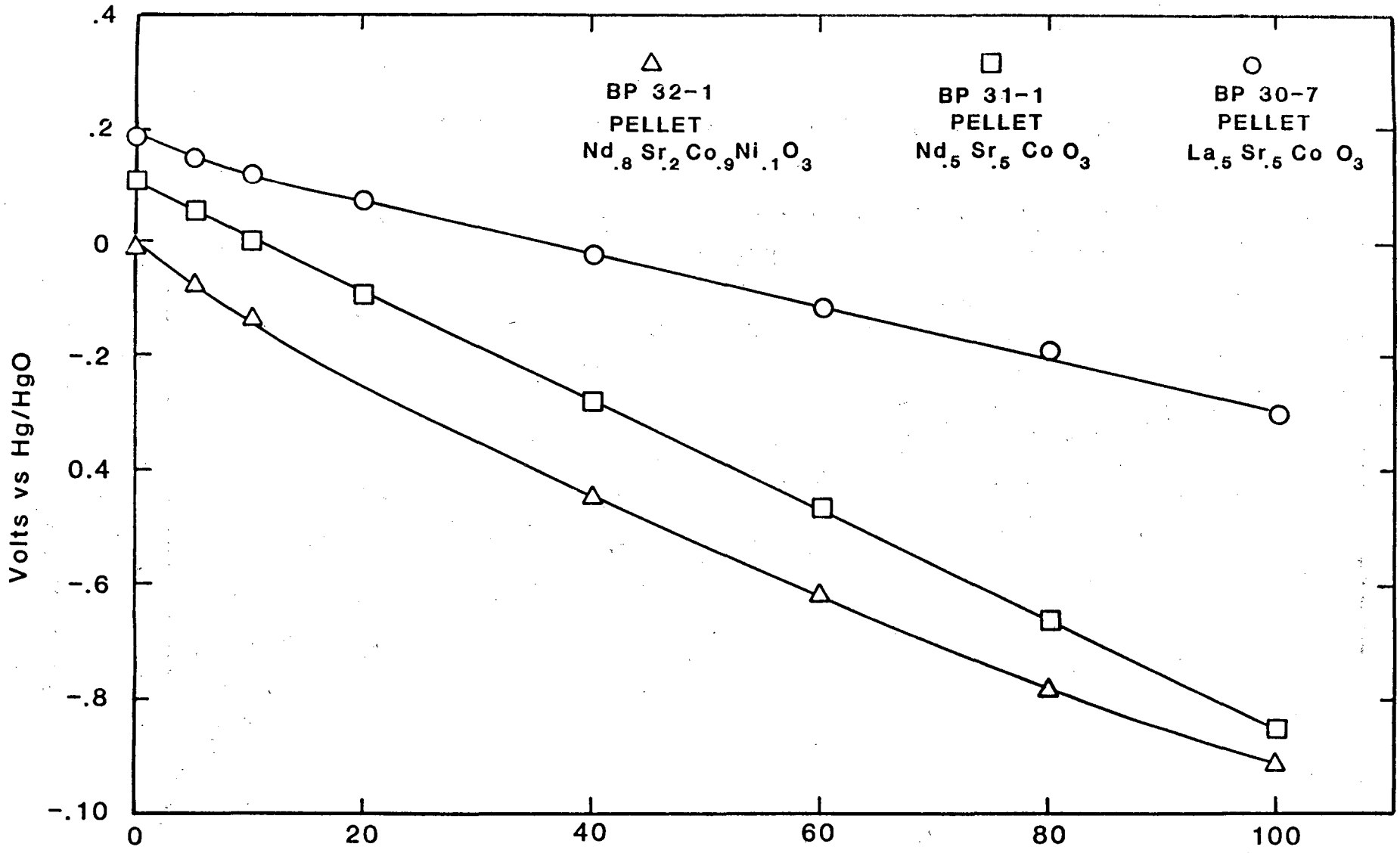

O_2 Reduction Polarization Curves- Pellets, Pure O_2 atm

FIGURE 15

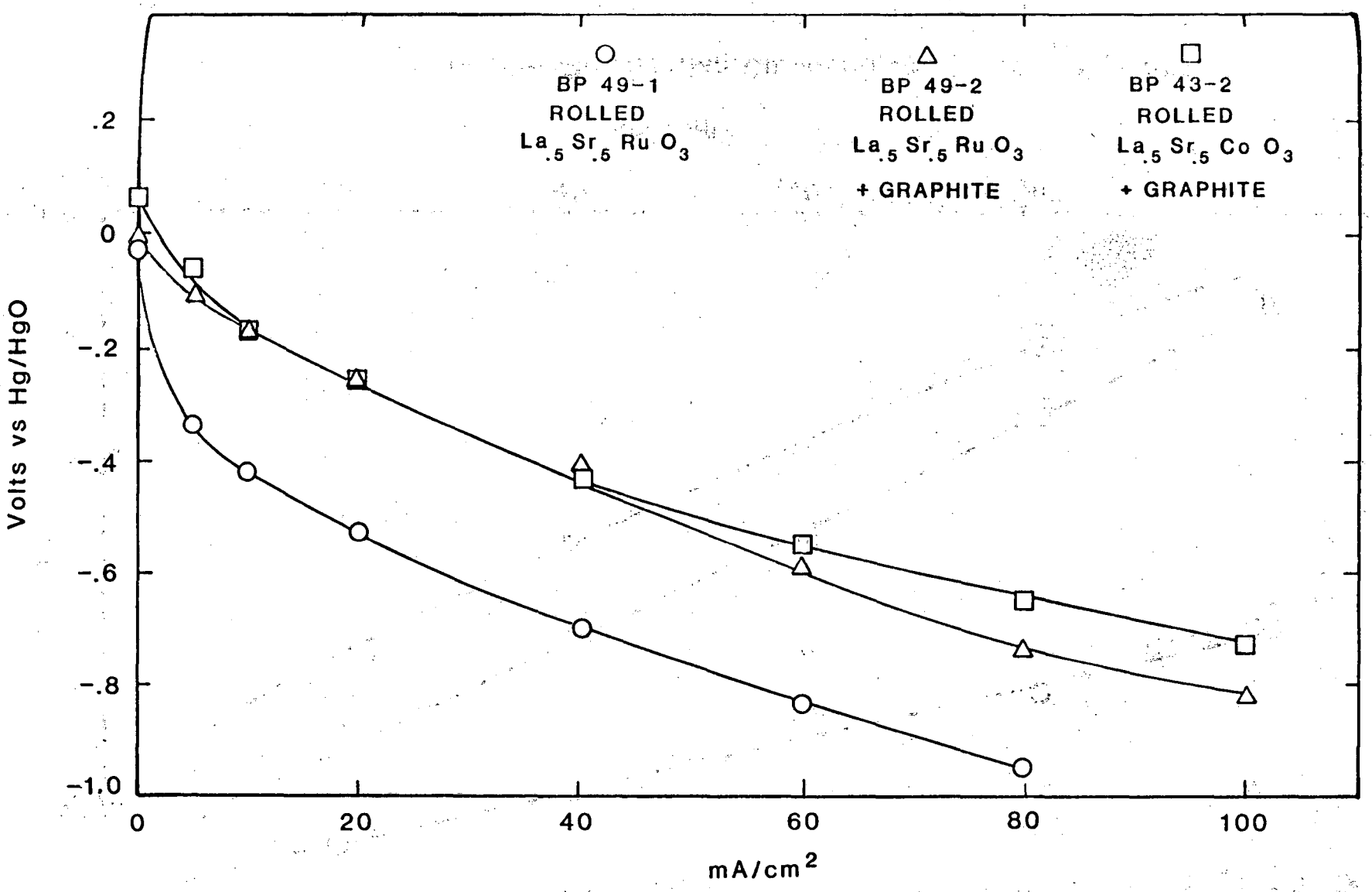

O_2 Reduction Polarization Curves- Roll Bonded, Pure O_2 atm

FIGURE 16

Performance characteristics of some selected representative samples are discussed below and the changes in polarization values with cycling are presented in Figure 17 through 23.

$Nd_{.5}$ $Sr_{.5}$ $Co\ O_3$: In the reduction mode, polarization started at 400 millivotls and increased steadily on cycling. The deterioration was rapid after 230 cycles and the potential reached 800 millivolts. This is also reflected in the oxygen evaluation mode which shows a similar increase (Figure 17).

$Nd\ Co\ O_3$: This electrode exhibits steady and stable potentials both in the anodic and cathodic modes. Polarization values during the first 400 cycles are 600 and 360 millivolts for oxygen evolution and reduction respectively (Figure 18).

$La\ Co\ O_3$: The potentials at the beginning of cycling were higher but the electrode appears to improve with cycling. After 450 cycles values of polarization decreased by 100 millivolts. The reason for this phenomenon is not known at this time (Figure 19).

$La_{.5}$ $Sr_{.5}$ $Ru_{.5}$ $Co_{.5}$ O_3: Despite the good conductivity of $La\ Ru\ O_3$, performance of this perovskite was slightly inferior to that of $La_{.5}$ $Sr_{.5}$ $Co\ O_3$ and addition of ruthenium does not appear to have any beneficial effects (Figure 20).

$La_{.5}$ $Sr_{.5}$ $Co\ O_3$: Electrodes prepared with this perovskite continue to exhibit the best performance on cycling. After 650 charge-discharge cycles, the potential remains at a steady value of 300 millivolts. Polarization for reduction

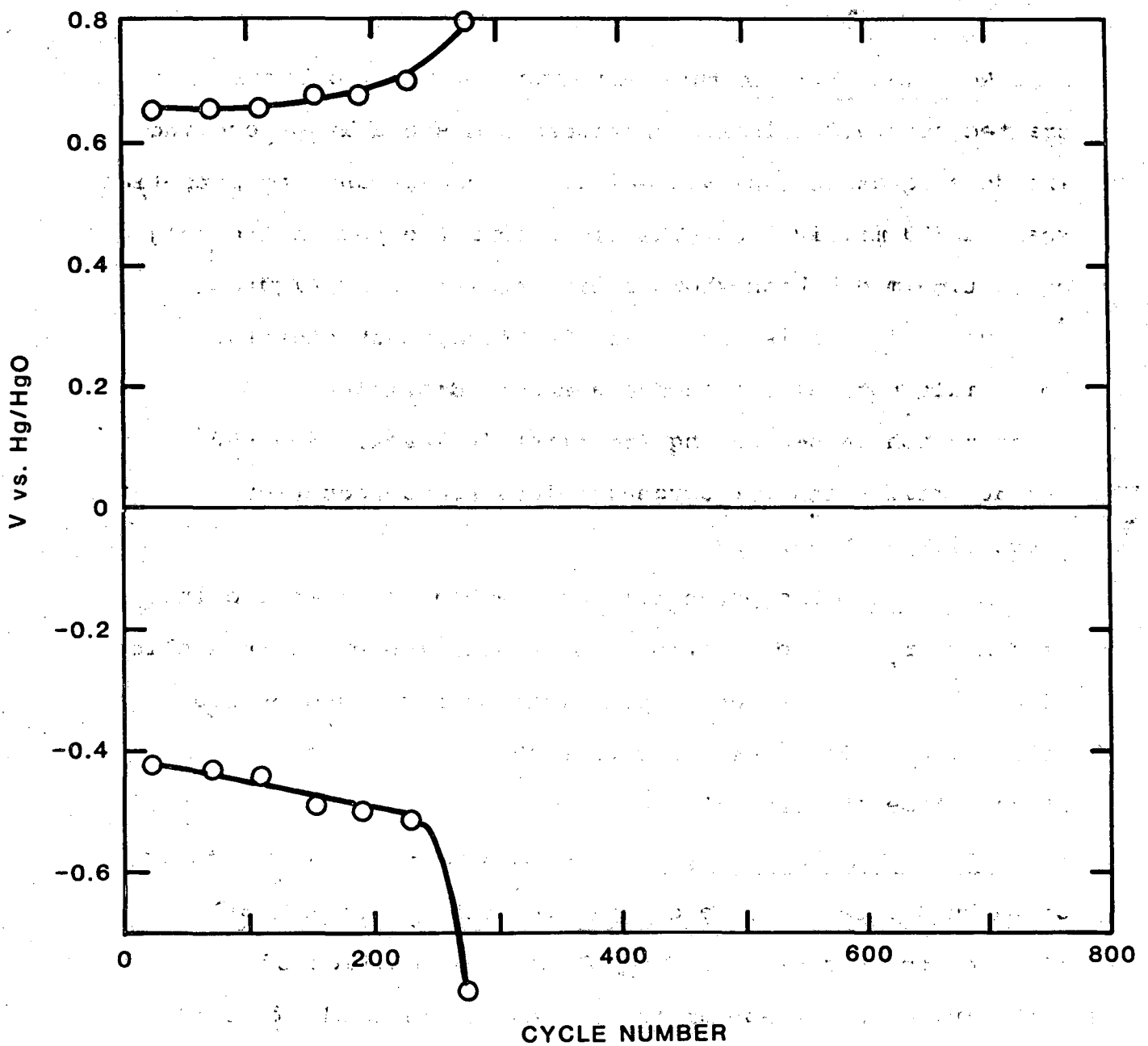

FIGURE. 17 POTENTIALS, BIFUNCTIONAL CYCLING-$Nd_{.5}Sr_{.5}CoO_3$

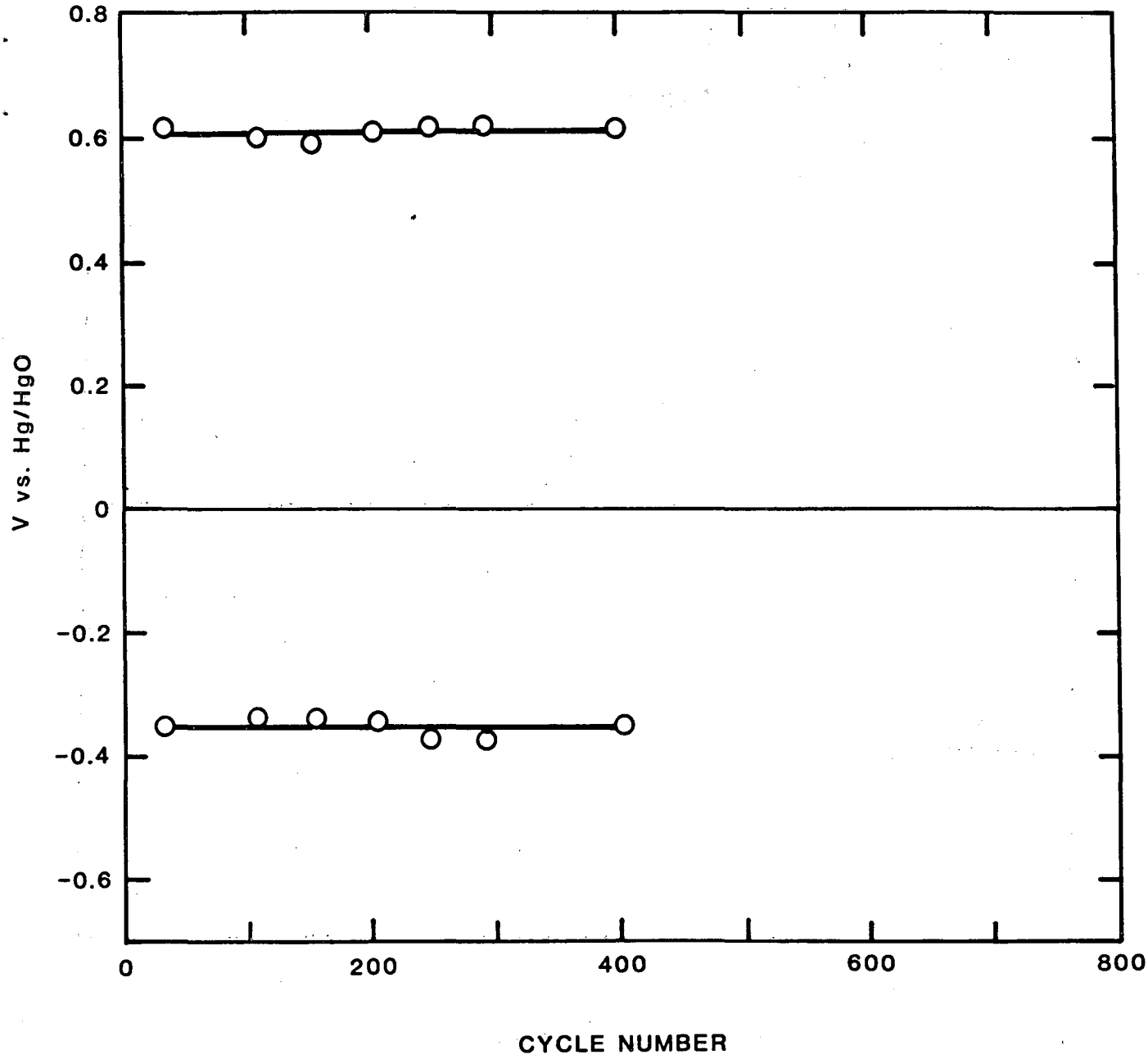

FIGURE. 18 POTENTIALS, BIFUNCTIONAL CYCLING-Nd CoO_3

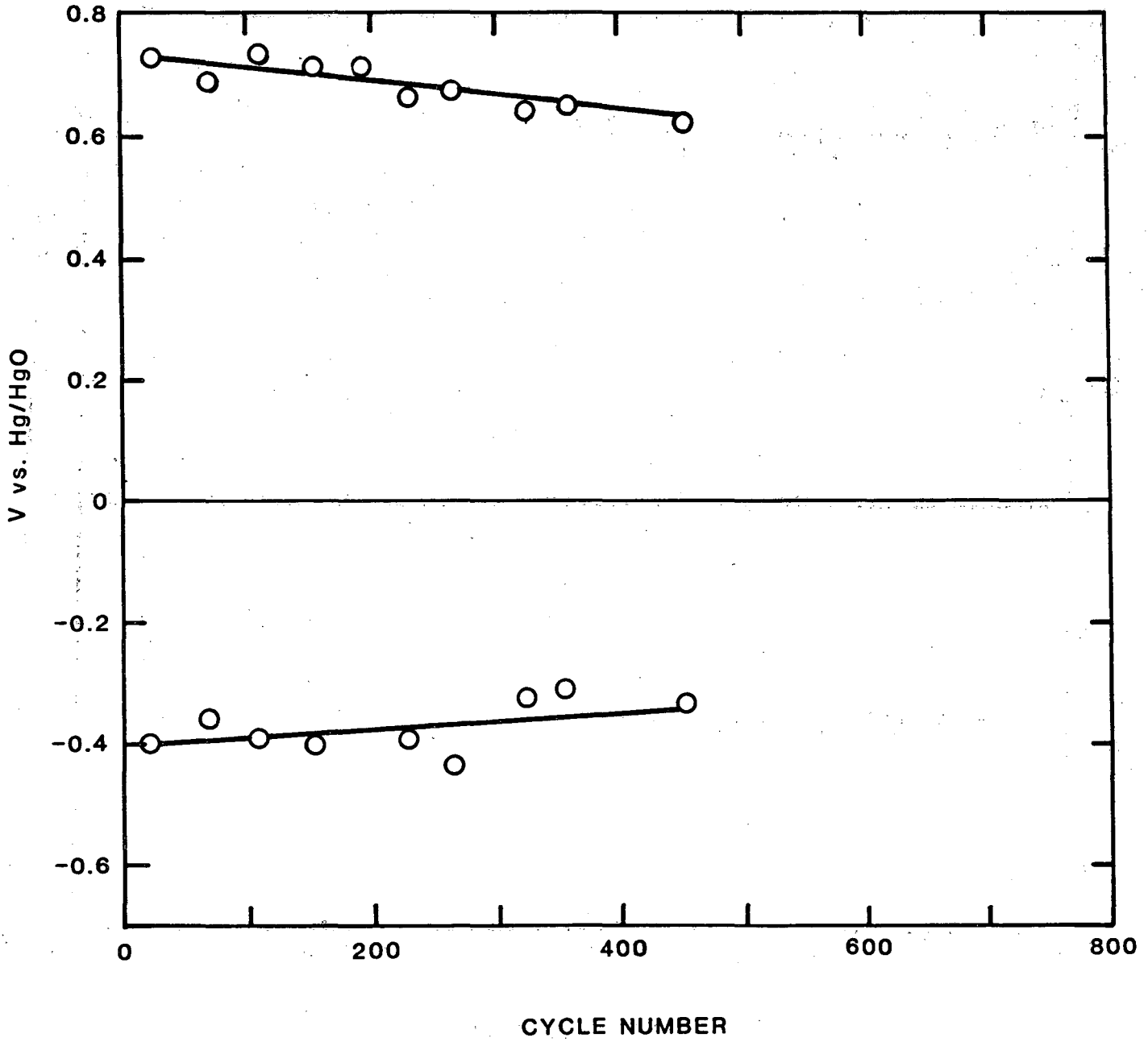

FIGURE. 19 POTENTIALS, BIFUNCTIONAL CYCLING-La CoO_3

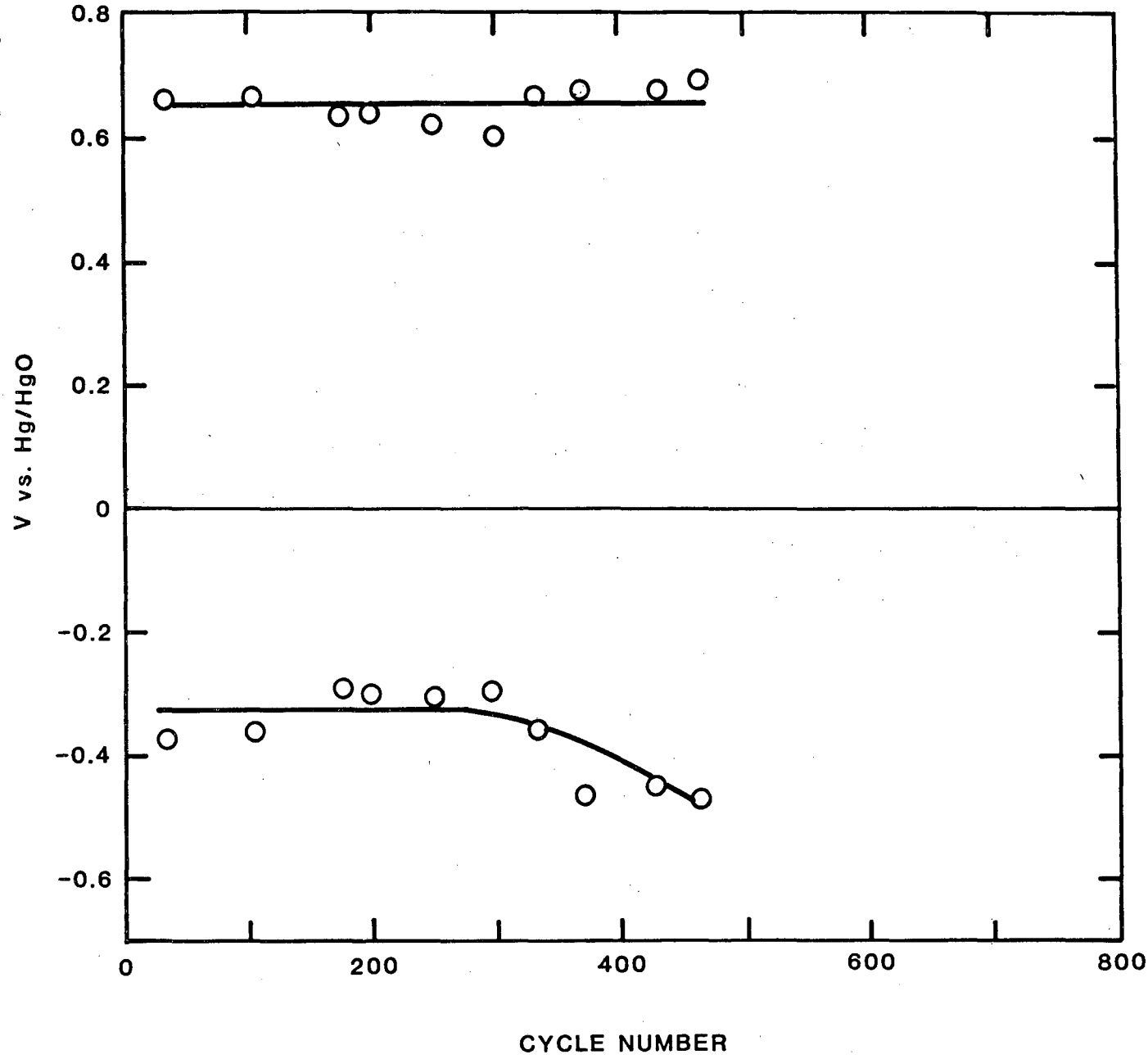

FIGURE. 20 POTENTIALS, BIFUNCTIONAL CYCLING-$La_{.5}Sr_{.5}Ru_{.5}Co_{.5}O_3$

was 400 millivolts in the beginning and after 100 cycles it dropped to 300 millivolts, a value at which the potential remained constant. It appears that the electrode required approximately four days for all the pores to be wetted uniformly and reach equilibrium (Figure 21).

Another electrode was prepared by adding nickel powder (5% by weight) to a perovskite of the same composition to see if this would result in improving conductivity and, therefore, the polarization. The test results indicate that the addition of nickel powder has no effect on the performance. After 700 cycles the electrode started to deteriorate and the polarization value has increased to 450 millivolts on the 900th cycle (Figure 22). For purposes of comparison, data for the bifunctional gold electrode is shown in Figure 23.

4.2.4 ELECTRODE PERFORMANCE - CONTINUOUS CATHODIC MODE

Four of the electrodes were tested on a continuous O_2 reduction mode at 20 mA/cm² to investigate decay with time. Since these tests did not require bifunctional operation, test electrodes were first prepared without the O_2 evolution layer. Due to the hydrophobic nature of the catalyst layer, satisfactory contact in the gas-solid-liquid interface was difficult to achieve resulting in a higher IR drop. It was therefore decided to incorporate a hydrophilic nickel layer to the test sample.

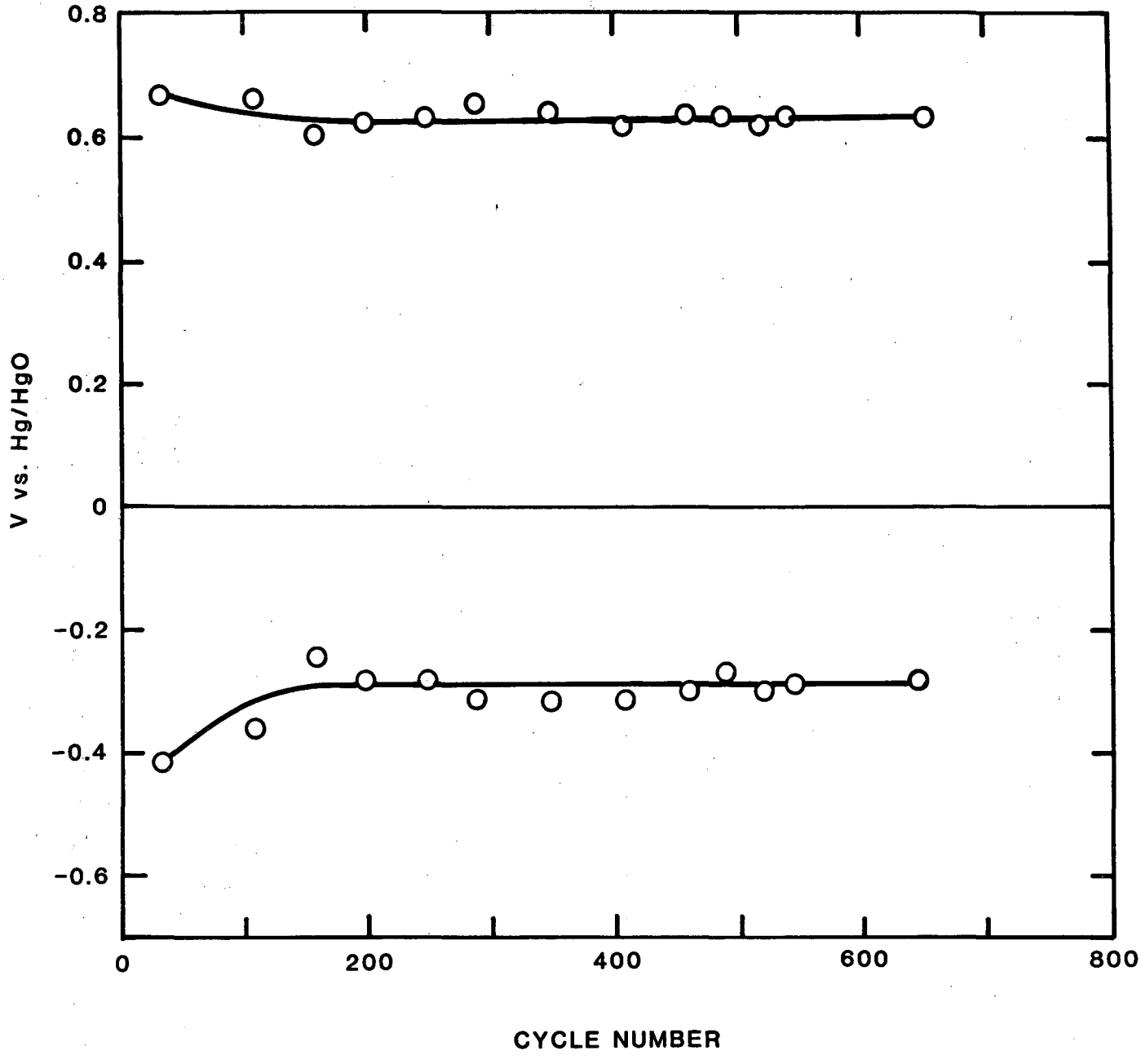

FIGURE. 21 POTENTIALS, BIFUNCTIONAL CYCLING-$La_{.5}Sr_{.5}CoO_3$

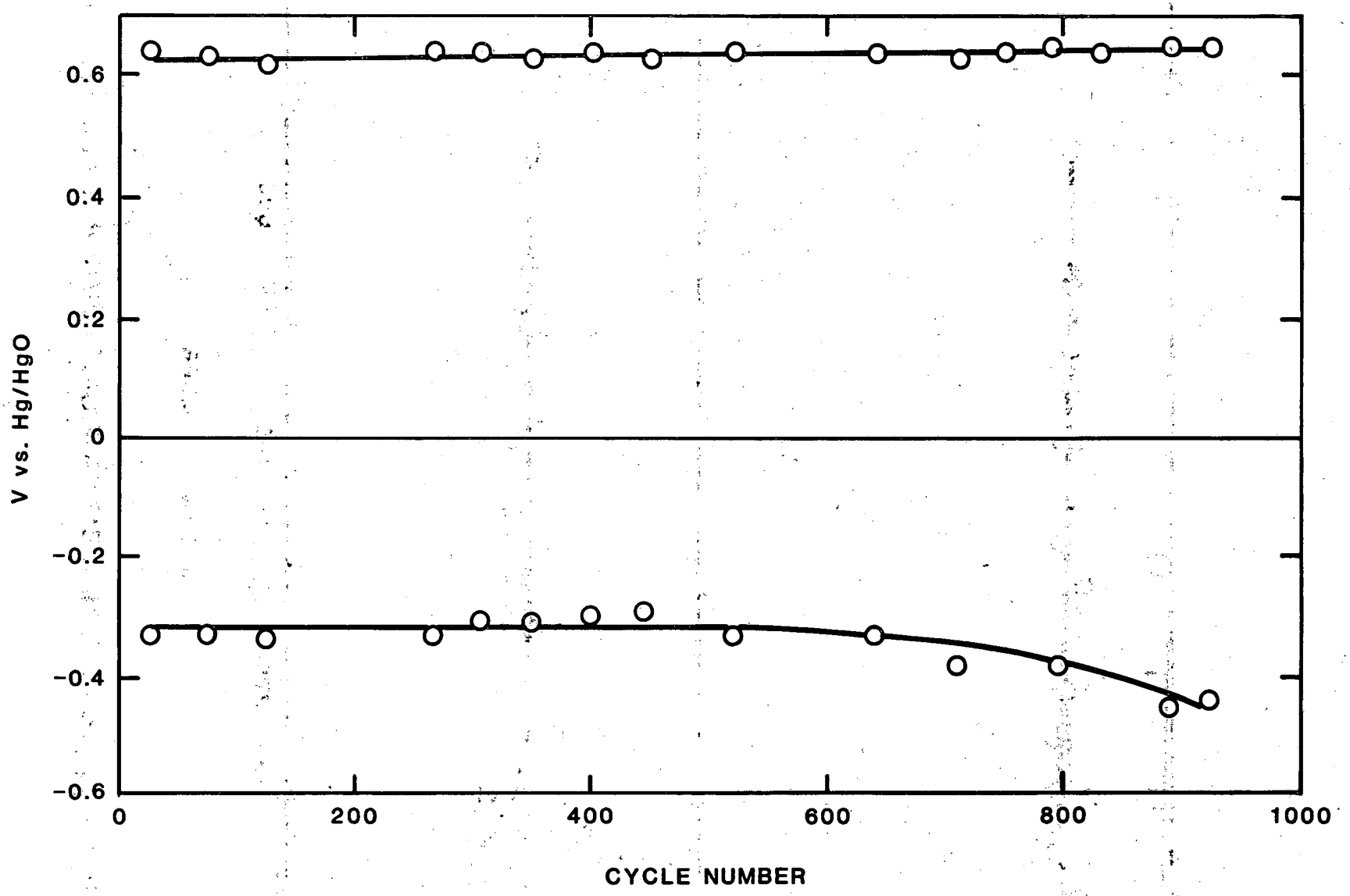

FIGURE 22 POTENTIALS, BIFUNCTIONAL CYCLING - $La_{.5}Sr_{.5}CoO_3$ - 5% Ni 287

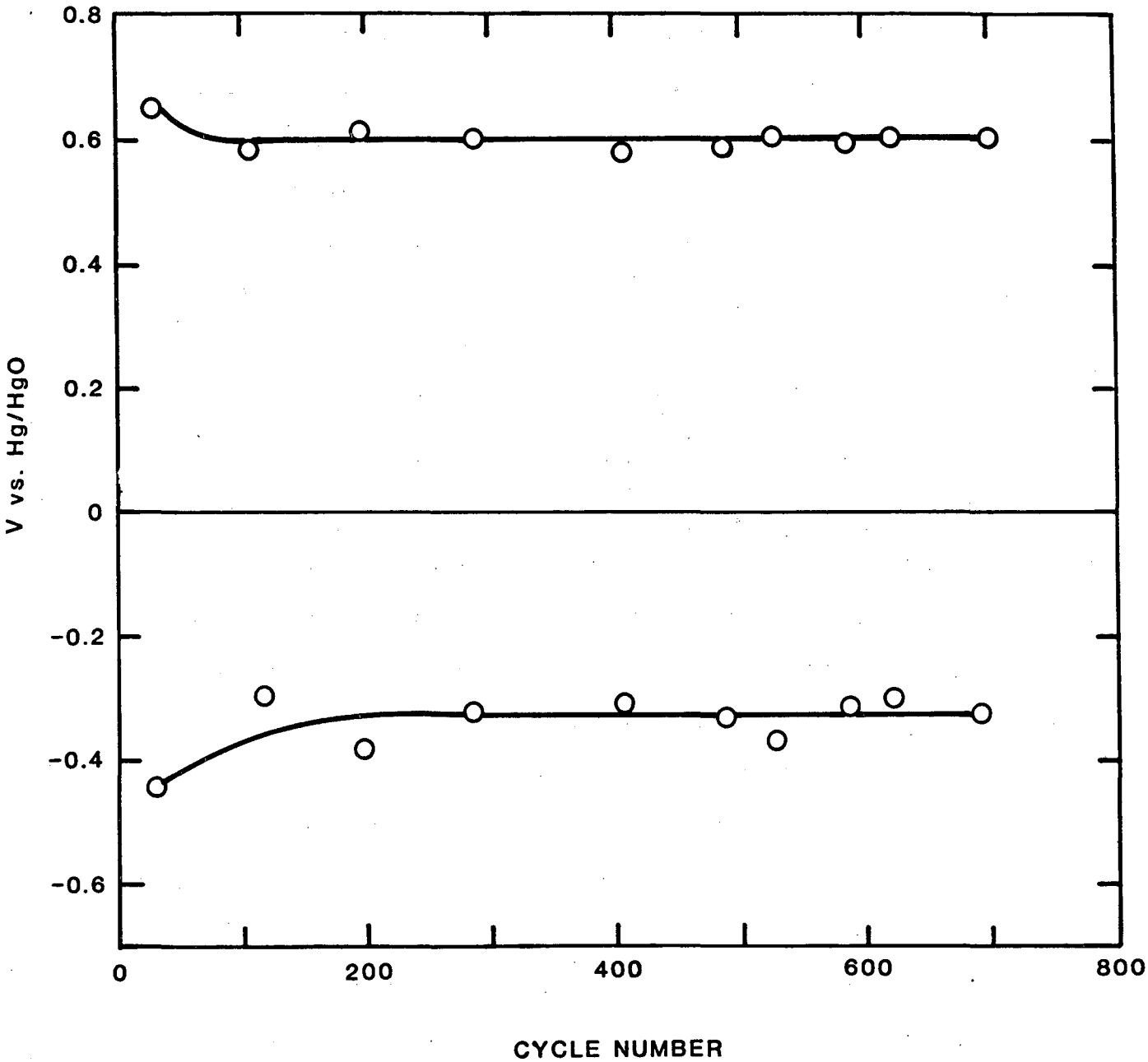

FIGURE. 23 POTENTIALS, BIFUNCTIONAL CYCLING-GOLD, CONTROL

La Ni O_3: After 700 hours of operation without nickel layer, the test was interrupted, electrode removed, nickel layer was pressed on and tests resumed. An improvement in polarization was noticed immediately and the electrode exhibited constant potential for an additional 600 hours after which polarization started to increase. (Figure 24)

$La_{.5}$ $Sr_{.5}$ Co O_3: This electrode was tested without nickel layer for 1800 hours and results show continuous deterioration from the beginning. Another sample of the same composition was tested with a nickel layer. This has, to date, undergone 1600 hours and there is no evidence of any increase in polarization. (Figure 25)

$Nd_{.5}$ $Sr_{.5}$ Co O_3: Performance of this electrode is very similar to the one in which the Nd was replaced by La. However, when tested under cycling conditions, the electrode prepared with $Nd_{.5}$ $Sr_{.5}$ Co O_3 did not perform well. The reason for this anomaly requires further investigation. (Figure 26)

The half-cell potentials of these electrodes are presented in Figures 24, 25 and 26.

4.2.5 ELECTRODE PERFORMANCE - CONTINUOUS ANODIC MODE

Work was started in the final quarter to study the preparation and performance of the O_2 evaluation layer of the bifunctional electrode. In addition to the perovskite electrode containing a nickel layer, four other compositions were prepared and tested.

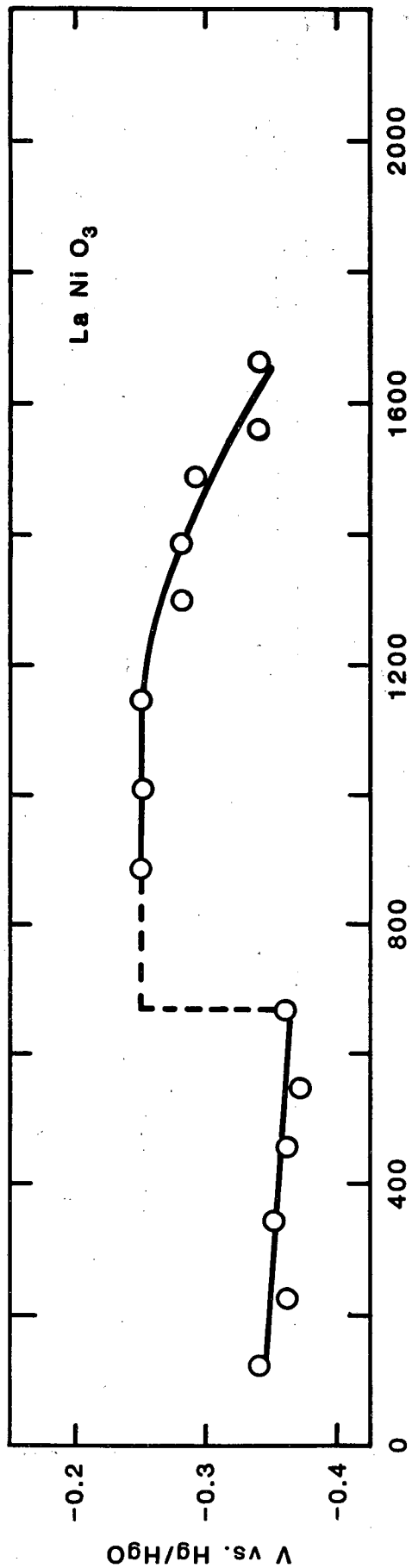

FIGURE 24 HALF-CELL POTENTIALS - CONTINUOUS O_2 REDUCTION

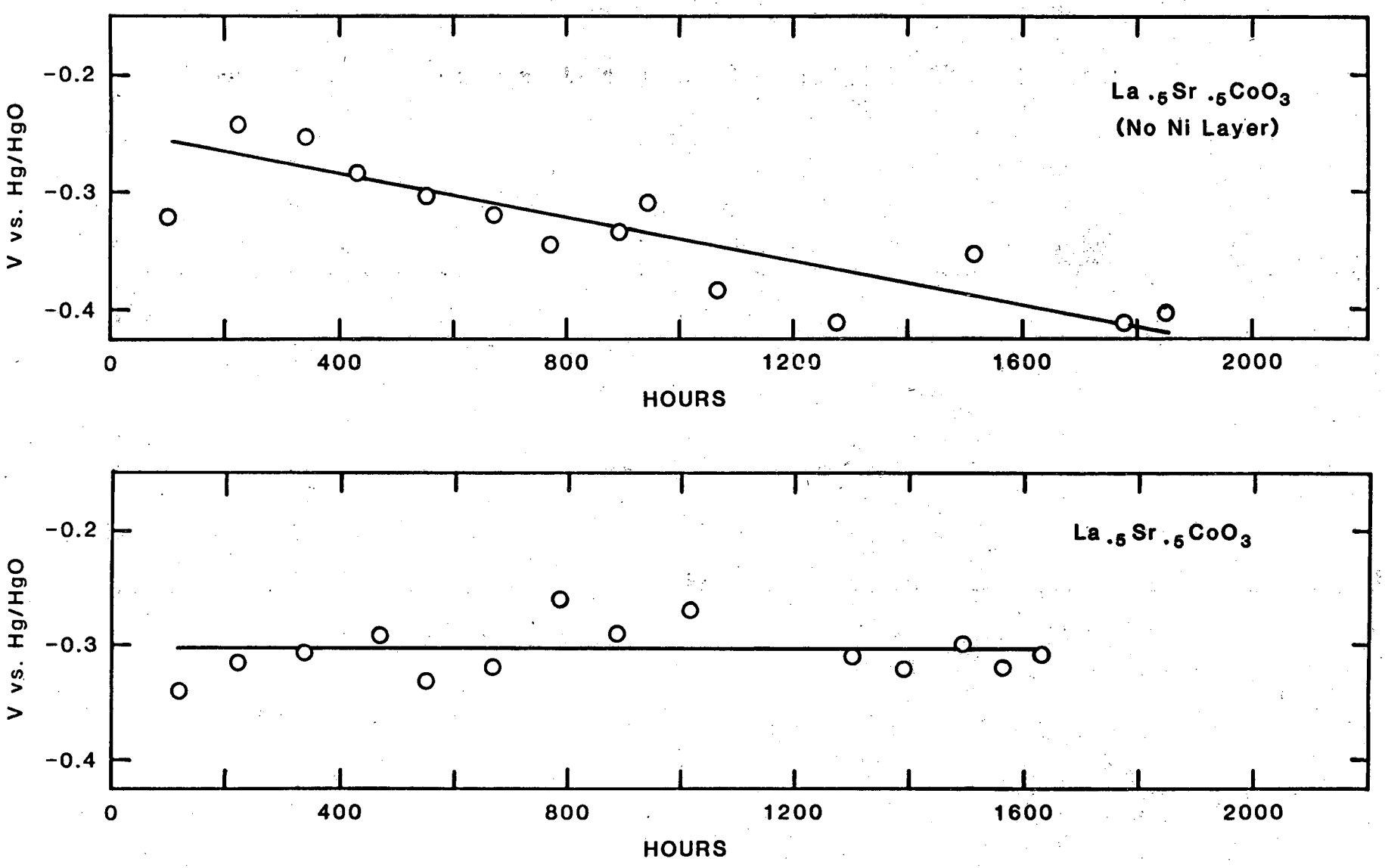

FIGURE. 25 HALF-CELL POTENTIALS-CONTINUOUS O_2 REDUCTION

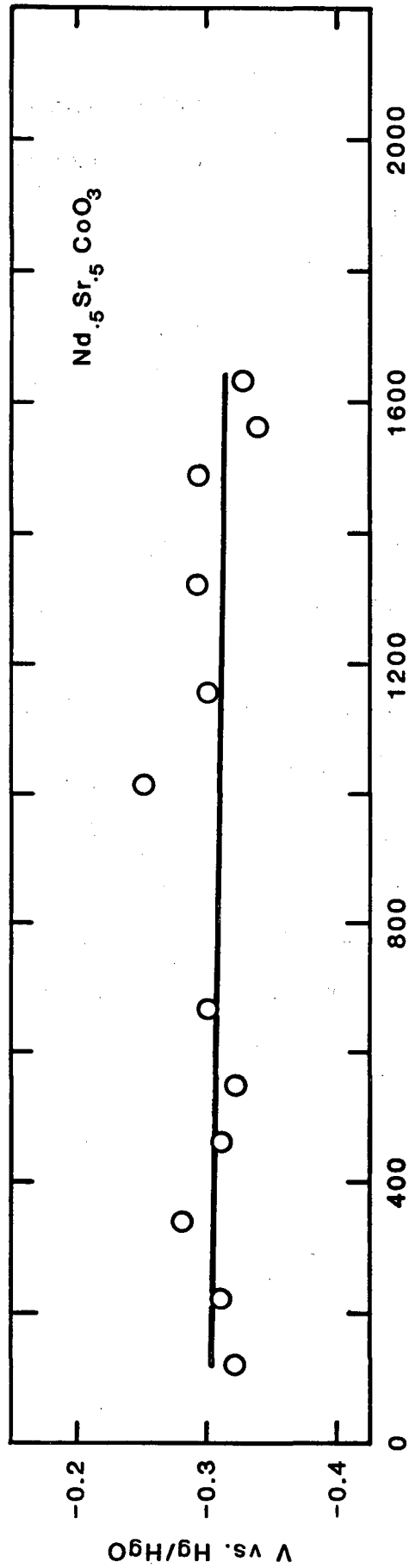

FIGURE 26 HALF-CELL POTENTIALS - CONTINUOUS O_2 REDUCTION

Electrodes containing nickel exmet and nickel 287 without the catalyst layer showed high polarization values of 0.8 and 1.0 volts respectively at 10 mA/cm^2. When a perovskite catalytic layer was added to the nickel layer, the polarization dropped to 640 millivolts. Even in the absence of the nickel layer, a sample of perovskite gave a comparable value of 650 millivolts thereby indicating its ability to support O_2 evolution.

Work was also started on the study of various Ni/Mo alloys. The first sample was prepared by reduction of salts in an atmosphere of hydrogen at 300°C. The composition of the powder was 95% nickel and 5% molybdenum by weight. Using this powder, an electrode was prepared and tested in the anodic mode. After 400 hours of continuous operation the potential was 700 millivolts. Addition of molybdenum to nickel appears to lower its polarization.

The experimental results are summarized in Table 6.

TABLE 6

POLARIZATION DATA FOR O_2 EVOLUTION

S #	COMPOSITION	HOURS	Avg. Volts vs. Hg/HgO @ 10 mA/cm^2	REMARKS
1	Ni exmet 5 Ni 7/0	408	.831	
2	Ni 287	408	1.000	
3	5% Mo + 95% Ni	408	.700	Reduced in H_2 @ 300°C
4	$La_{.5}Sr_{.5}CoO_3$	864	.644	Perovskite + std. Ni layer
5	"	288	.653	Perovskite, No Ni layer

5.0 Task III - Zinc Air for EV Battery - an engineering analysis.

A detailed engineering analysis of the zinc-air battery system at one of the potential candidates to power the electric vehicles was performed and a report has already been submitted. In order to avoid duplication only an outline of the work performed under this task is given below.

The distinguishing feature of the zinc-air system is its flexibility; in addition to the convential method of classical recharging, options such as mechanically refuelable and circulating systems are available. The report examines many possible alternatives and compares the performance, cost, convenience and complexity of each of the schemes.

The following zinc-air battery systems are examined in this analysis:

Mechanically Refuelable

Electrically Rechargeable

Circulating Electrolyte

Circulating Slurry

In addition, where applicable, alternate methods of operation are given. For example, the electrically rechargeable system can operate either as an open air or a sealed oxygen system and the circulating slurry system can be designed with on-board electrolysis or regeneration can be done externally.

Several possible operating schemes of the zinc-air system are analyzed and the advantages and disadvantages of each of the schemes are discussed. Assuming a vehicle weight of 2000 lb. the

material requirements, weight of battery and cost comparisons are calculated. It must be recognized that the cost calculations are empirical in nature and based on certain assumptions with the objective of comparing the cost effectiveness of the different schemes; accordingly the cost figures are not to be construed as actual values for a practical operating system.

Critical parameters such as weight, energy, cost and range of the different systems are compared on the basis of constant weight, constant cost and constant energy.

Finally, this analysis also includes performance projections and identifies specific areas of development efforts that will be required in order to transform zinc-air batteries for EV propulsion from the conceptual to a practical and cost-effective operating phase.

6.0 SUMMARY AND CONCLUSIONS

6.1 Tasks I and II

During the final quarter, efforts were directed more towards completion of on-going experiments rather than investigating new areas and catalysts. However, due to limitations in time and funding, the expended efforts were insufficient to complete all tests.

Testing of electrodes in half-cells were continued with monitoring of potentials against Hg/HgO reference electrode. Tests were terminated when polarization exceeded 500 millivolts. In addition to testing of electrodes on continuous cathodic and bifunctional modes of operation, tests were started to characterize electrode performance when operated on a continuous oxygen evolution regime.

Bifunctional Mode

Electrodes fabricated with perovskites of the following compositions were tested in the bifunctional operating mode:

$La_{.5}\ Sr_{.5}\ Co\ O_3$
$La_{.5}\ Sr_{.5}\ Ru_{.5}\ Co_{.5}\ O_3$
$La\ Co\ O_3$
$La_{.9}\ Nd_{.1}\ Ni\ O_3$
$La_{.5}\ Sr_{.5}\ Co\ O_3$ + Ni 287
$La\ Ni\ O_3$
$Nd_{.5}\ Ca_{.5}\ Co_{.8}\ Ni_{.2}\ O_3$

Electrodes prepared with $La\ Co\ O_3$ and $La_{.9}\ Nd_{.1}\ Ni\ O_3$ gave 790 and 456 cycles respectively to failure i.e. polarization

exceeded 500 millivolts. All other test electrodes were still performing well at the time of termination of tests.

In a continuous O_2 reduction mode, electrodes containing the following perovskites were tested.

$La\ Co\ O_3$
$Nd\ Co\ O_3$
$Nd._5\ Sr._5\ Co\ O_3$
$La\ Ni\ O_3$
$La._9\ Nd._1\ Ni\ O_3$
$La._5\ Sr._5\ Co\ O_3$
$Nd._5\ Ca._5\ Co._8\ Ni._2\ O_3$

None of these samples had failed when tests were stopped. Electrode fabricated with $La\ Ni\ O_3$ had been on test for the longest time (2,700 hours) and the average polarization was 340 millivolts at 20 mA/cm^2.

During the final quarter, work on evaluating O_2 evolution was started. The O_2 generation layer consisted of a Ni-Mo alloy and no improvements were noticed compared to the standard Ni layer.

However, when a perovskite layer was added to the O_2 evolution layer to constitute a bifunctional electrode, the O_2 generation potential improved by about 200 millivolts at a current density of 10 mA/cm^2.

Perovskite of the composition $La_{.5}\ Sr_{.5}\ Co\ O_3$ exhibited the most stable performance of all three regimes--bifunctional, O_2 reduction and O_2 generation. Towards the end of the program, a new perovskite of the compositon $Nd_{.5}\ Ca_{.5}\ Co_{.8}\ Ni_{.2}\ O_3$ was synthesized and tested.

Its performance was comparable to $La_{.5}Sr_{.5}CoO_3$ in the bifunctional mode and was actually better in the continuous O_2 reduction mode. The tests could not be carried to completion and had to be stopped after 280 cycles of bifunctional testing and 1000 hours of operation in a continuous cathodic mode. In the continuous O_2 reduction mode, without a nickel layer, polarization was about 300 millivolts. After 100 hours, a nickel layer was added to the same electrode and the polarization was less by about 100 millivolts. This is probably due to the fact that the hydrophobicity of the O_2 reduction layer prevented proper contact at the gas-solid-liquid interface. The break in Figure 27 shows the improvement when the nickel layer was added.

Polarization values of this electrode are shown in Figures 27 and 28.

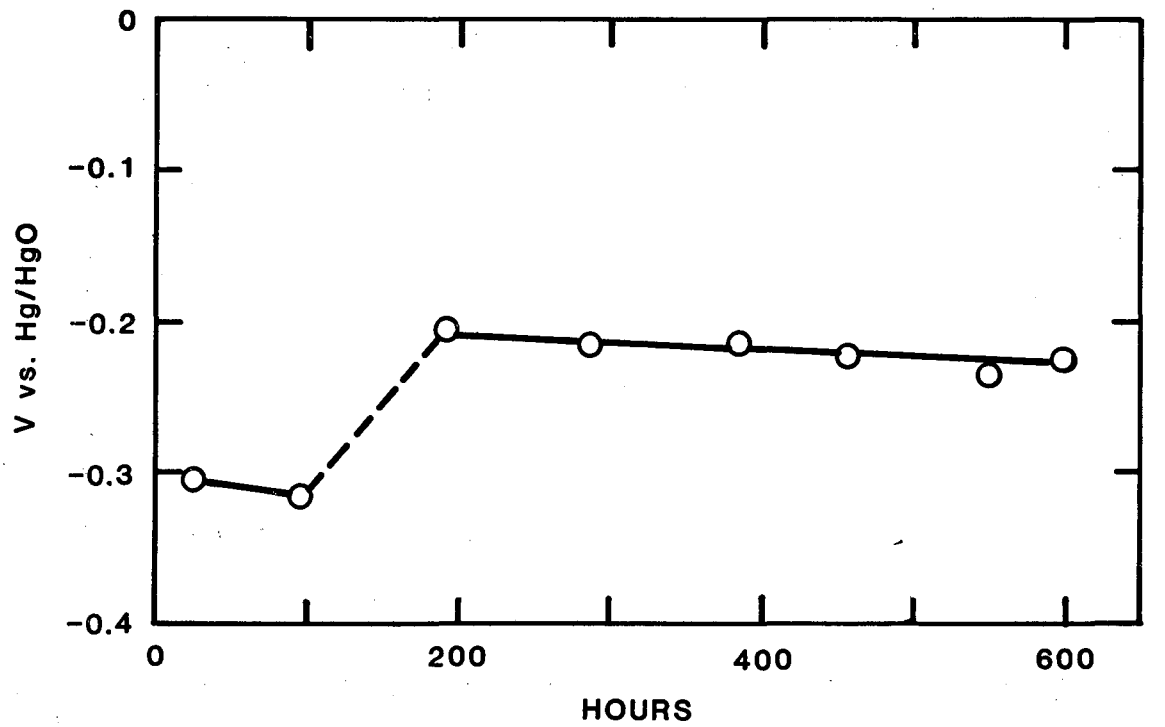

FIGURE 27 HALF-CELL POTENTIALS CONTINUOUS O_2 REDUCTION - $Nd_{.5}\ Ca_{.5}\ Co_{.8}\ Ni_{.2}\ O_3$

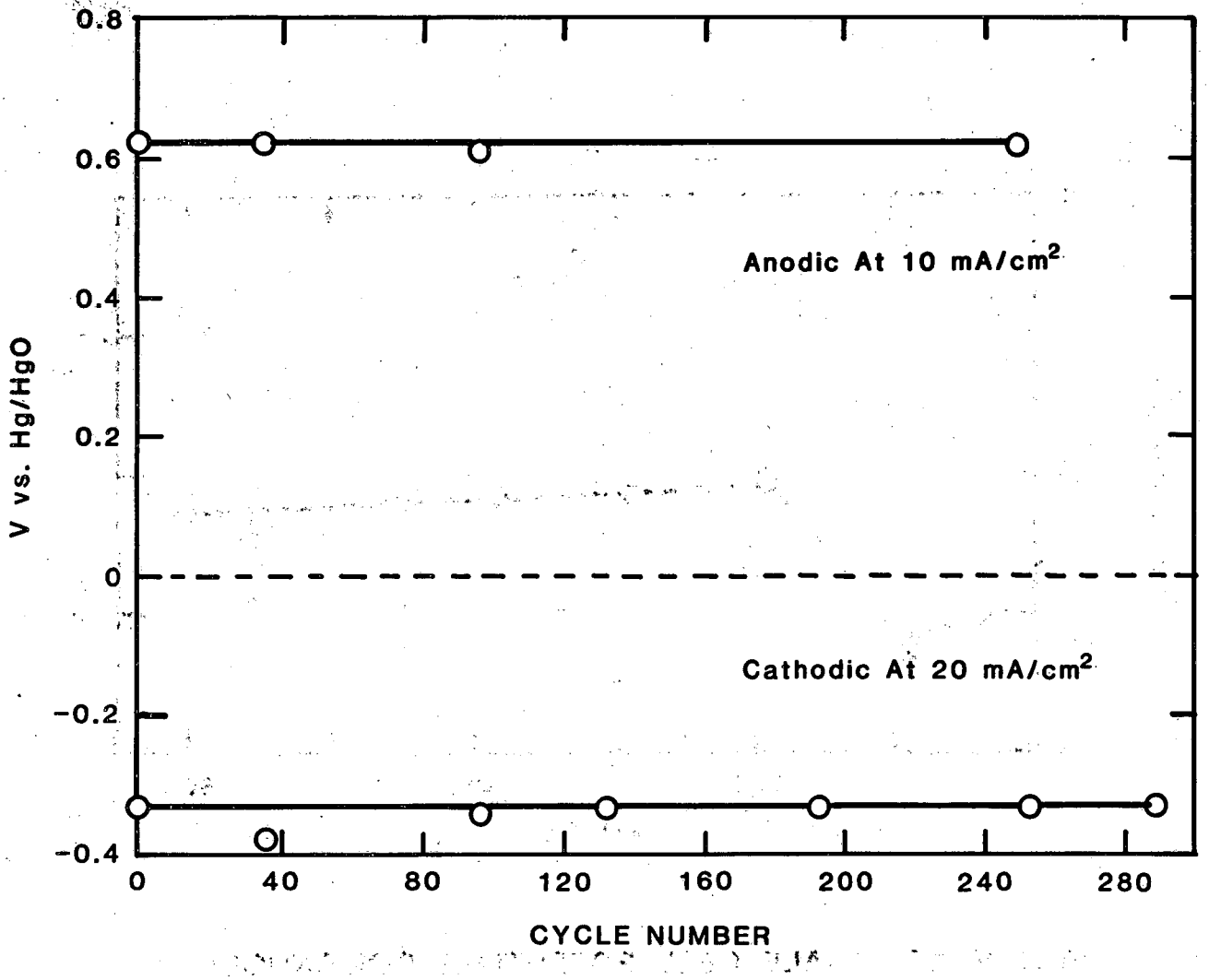

FIGURE 28 POTENTIALS, BIFUNCTIONAL CYCLING $Nd_{.5}\ Ca_{.5}\ Co_{.8}\ Ni_{.2}\ O_3$

6.2 TASK III

From the analysis presented in the zinc-air report, it is clear that the zinc-air battery for electric vehicles offers a variety of operating alternatives compared to the other batteries. Each of the operating schemes has its own distinct merits and demerits; accordingly, the final choice would be dependent upon factors such as type of driving, range and speed, ease of charging, system problems and cost.

The five different systems examined are all intended to operate primarily in an urban environment. Depending on the system and basis of design, the estimated range of operation varies between 83 and 241 miles.

Even assuming a significant market penetration of 10%, electric vehicles of the future will be required to compete in a world dominated by internal combustion engines. It is imperative therefore, that energy and power densities be improved, current limitations must be overcome and efficiency of motor/controller/drive train systems be improved.

Despite the basic limitations inherent in battery systems, significant improvements in energy densities have been accomplished in recent years. Based on this, it is felt that practical energy densities in excess of 75 Wh/lb are achievable with zinc-air batteries. However, in order to reach this goal, more research and development efforts need to be expended on electrochemical research and systems management.

As a direct result of the R&D efforts of this program, the following technical presentation was made at the IECEC conference in 1985. A similar presentation was also made at the 7th Battery & Electrochemical Contractors' Conference.

S. Viswanathan and A. Charkey, "Bi-functional Oxygen Electrodes for Rechargeable Metal-Air Cells", Proceedings of the 20th IECEC, Vol. 2, August 1985.

X-RAY DIFFRACTION ANALYSIS

SAMPLE I.D.	ERC COMPOSITION	EDX ATOMIC %	XRD PHASE I.D.	CRYSTAL STRUCTURE
ZB-1	Co_3O_4	98 Co, 1 Ni	Graphite, Co_3O_4	Cubic
P5C	$La_{.5}Sr_{.5}Co\ O_3$	20 lA, 25 Sr, 55 Co, 1 Ni	La Co O_3	Rhombohedral
P8	La Ni O_3	46 la, 54 Ni	La Ni O_3	Rhombohedral
P20	$Nd_{.8}Sr_{.2}Co_{.9}Ni_{.1}O_3$	34 Nd, 7 Sr, 52 Co, 7 Ni	Nd Co O_3	Cubic

Energy dispersive x-ray analysis confirms bulk composition of material to be identical to ERC formulation. X-ray diffraction shows perfect match to patterns of known phases. No peak shift or variance in peak rates was observed. The addition of Sr to samples P5C and P20 did not affect the crystal structure of the cobalt oxides. ZB1 and P20 were found to match cubic phase patterns which indicated spinel formation.

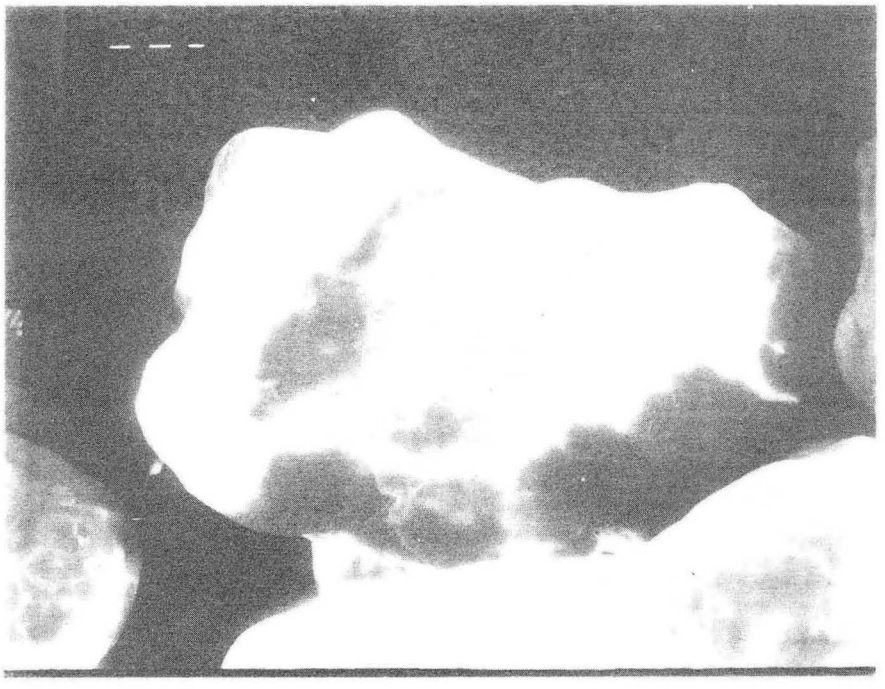

PTFE Teflon powder smallest particle
gold sputtering 30 sec
170X SEM

PTFE Teflon powder rolled
gold sputtered
100X SEM

Lonza graphite, gold sputtered, 30 sec
2000X SEM

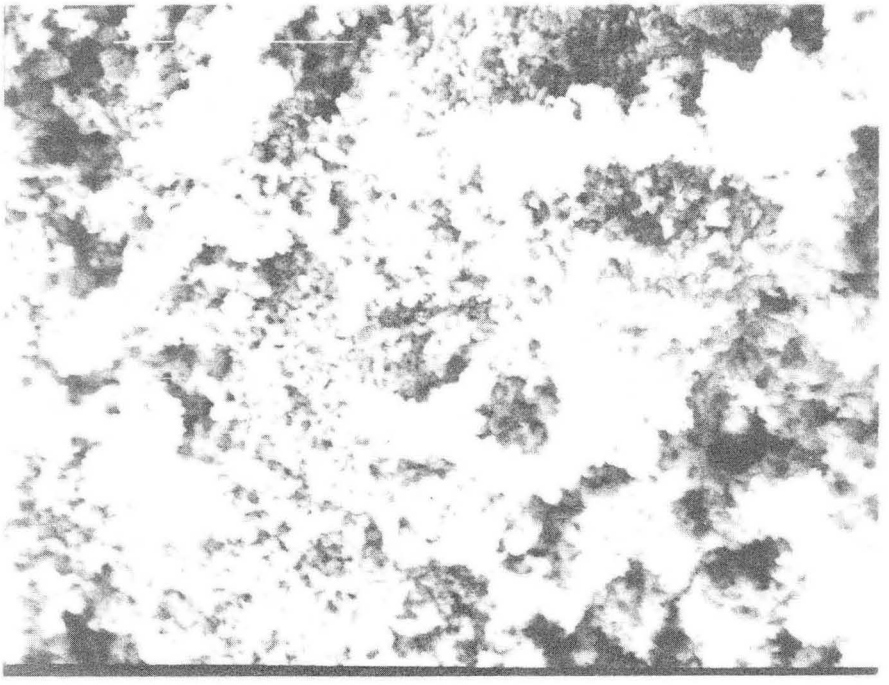

P50, gold sputtering, 30 sec
La Sr CoO

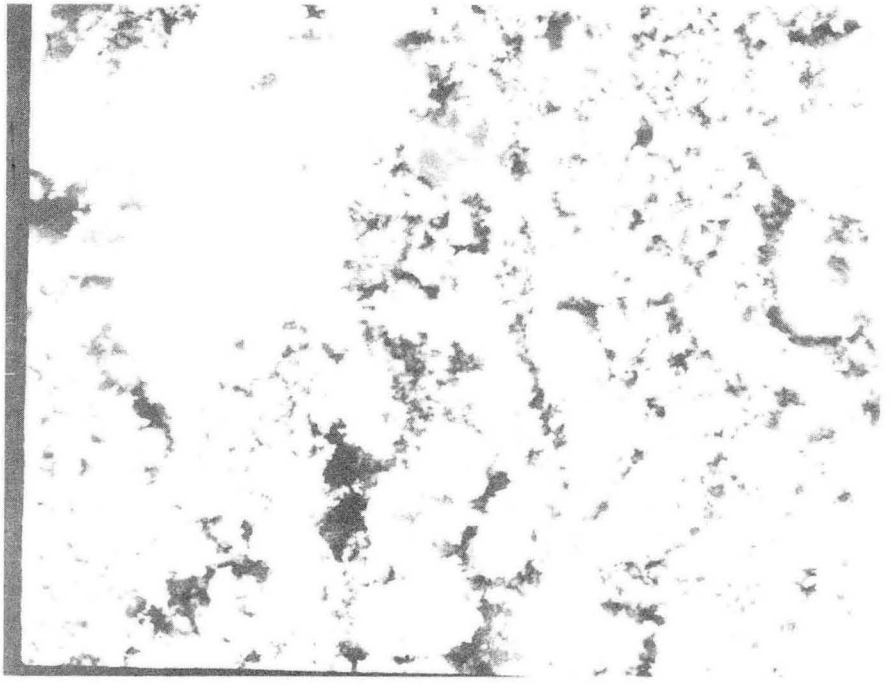

P48, 20Å
La Sr CoO

FRESH CATALYST LAYER

$La_{.5}Sr_{.5}CoO_3$ + Graphite + 25% TFE

New, BP30-8, 1000X SEM

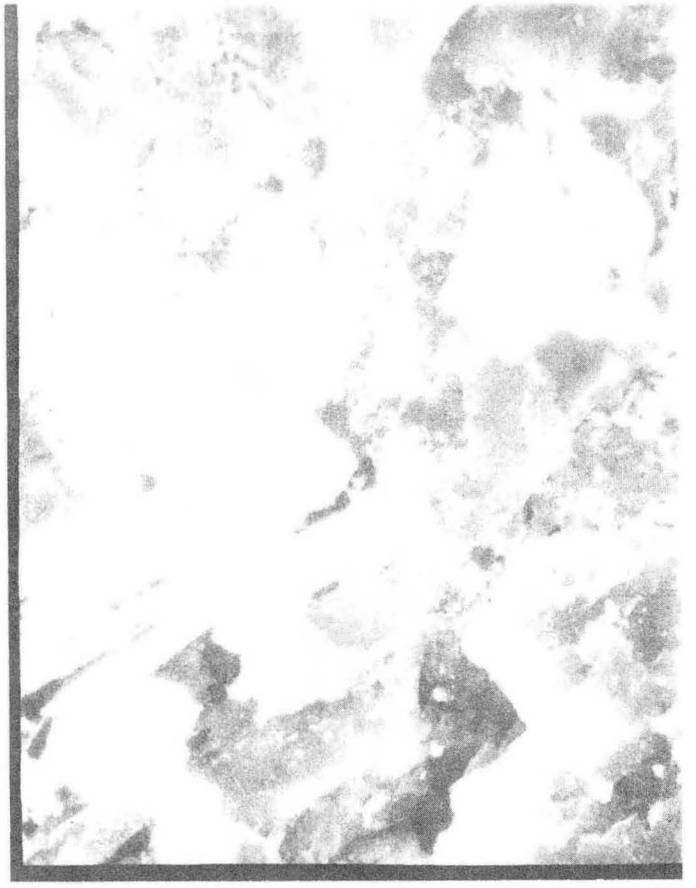

Used BP30-8, Air Side
1000X SEM

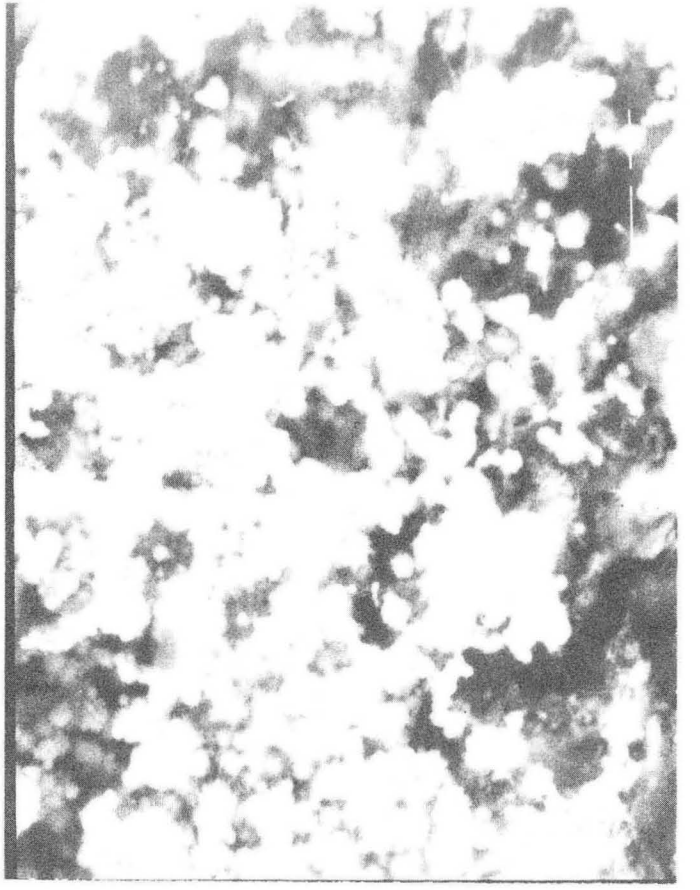

Used BP30-8, Electrolyte Side
1000X SEM

USED CATALYST LAYER

$La_{.5}Sr_{.5}CoO_3$ + Graphite + 25% TFE

This report was done with support from the Department of Energy. Any conclusions or opinions expressed in this report represent solely those of the author(s) and not necessarily those of The Regents of the University of California, the Lawrence Berkeley Laboratory or the Department of Energy.

Reference to a company or product name does not imply approval or recommendation of the product by the University of California or the U.S. Department of Energy to the exclusion of others that may be suitable.

LAWRENCE BERKELEY LABORATORY
TECHNICAL INFORMATION DEPARTMENT
UNIVERSITY OF CALIFORNIA
BERKELEY, CALIFORNIA 94720